AD-A151 225 A PLASMA INITIATION/FLOW CHAMBER TO STUDY CW LASER BEAMED ENERGY ABSORPTI..(U) ILLINOIS UNIV AT URBANA DEPT OF MECHANICAL AND INDUSTRIAL ENG.. H KRIER ET AL. 1/1

UNCLASSIFIED 01 MAR 84 UILU-ENG-84-4002 AFOSR-TR-85-0205 F/G 20/5 NL

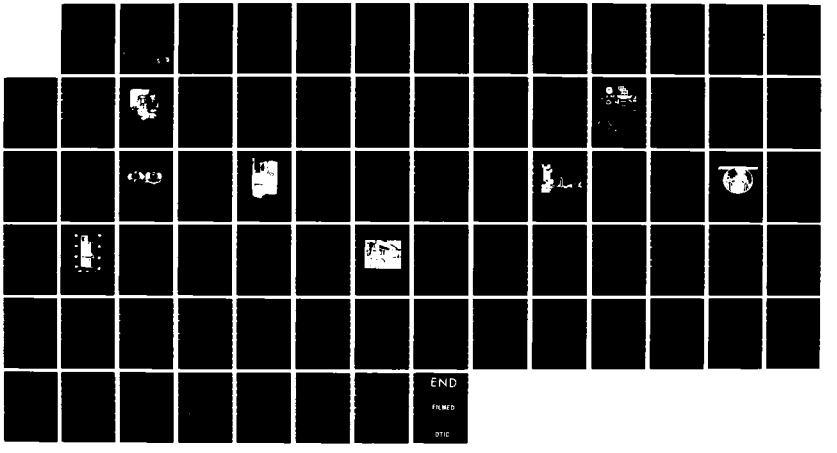

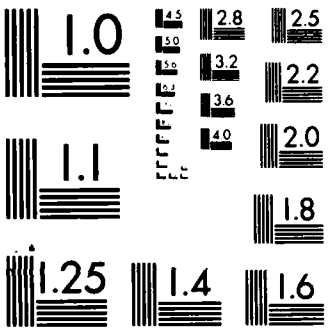

Department of Mechanical
and Industrial Engineering
University of Illinois at Urbana-Champaign
Urbana, IL 61801

Technical Report UILU ENG-84-4002

A PLASMA INITIATION/FLOW CHAMBER TO STUDY CW LASER BEAMED ENERGY ABSORPTION IN LIGHT GASES

Annual Technical Report

AFOSR Grant No. 83-0041

March 5, 1984

UNCLASSIFIED

SECURITY CLASSIFICATION OF THIS PAGE *(When Data Entered)*

REPORT DOCUMENTATION PAGE	READ INSTRUCTIONS BEFORE COMPLETING FORM
1. REPORT NUMBER **AFOSR-TR- 85-0205** 2. GOVT ACCESSION NO. AD-A151 225	3. RECIPIENT'S CATALOG NUMBER
4. TITLE *(and Subtitle)* A PLASMA INITIATION/FLOW CHAMBER TO STUDY CW LASER BEAMED ENERGY ABSORPTION IN LIGHT GASES	5. TYPE OF REPORT & PERIOD COVERED ANNUAL: 01 FEB 83-30 JAN 84
	6. PERFORMING ORG. REPORT NUMBER UILU-ENG-84-4002
7. AUTHOR(s) HERMAN KRIER, JYOTI MAZUMDER, RONALD J. GLUMB, TERRENCE D. BENDER, TODD J. ROCKSTROH	8. CONTRACT OR GRANT NUMBER(s) AFOSR-83-0041
9. PERFORMING ORGANIZATION NAME AND ADDRESS University of Illinois at Urbana-Champaign Department of Mechanical & Industrial Engineering 144 MEB; 1206 W. Green St.; Urbana, IL 61801	10. PROGRAM ELEMENT, PROJECT, TASK AREA & WORK UNIT NUMBERS 61102F 2308/A1
11. CONTROLLING OFFICE NAME AND ADDRESS AIR FORCE OFFICE OF SCIENTIFIC RESEARCH/NA BOLLING AFB DC 20332	12. REPORT DATE March 1, 1984
	13. NUMBER OF PAGES 74
14. MONITORING AGENCY NAME & ADDRESS(if different from Controlling Office)	15. SECURITY CLASS. (of this report) UNCLASSIFIED
	15a. DECLASSIFICATION/DOWNGRADING SCHEDULE

16. DISTRIBUTION STATEMENT *(of this Report)*

Approved for Public Release;
Distribution Unlimited

17. DISTRIBUTION STATEMENT *(of the abstract entered in Block 20, if different from Report)*

18. SUPPLEMENTARY NOTES

19. KEY WORDS *(Continue on reverse side if necessary and identify by block number)*

BEAMED ENERGY PROPULSION
CW LASER APPLICATION
Absorption of Electromagnetic Radiation

20. ABSTRACT *(Continue on reverse side if necessary and identify by block number)*

This report summarizes the research work that has been done in the past year, investigating the use of laser-sustained plasmas for propulsion applications. One focus of the research is the initiation of plasmas in inert gases using metal targets and metal vapor seedants. Another is to define the operating characteristics of the dual-flow design by measuring temperatures, number densities, and global absorption. A pressure chamber has been built to permit observations of the plasma under wide ranges of pressure, flow conditions, and

DD FORM 1 JAN 73 1473

UNCLASSIFIED

SECURITY CLASSIFICATION OF THIS PAGE *(When Data Entered)*

ANNUAL TECHNICAL REPORT

No. UILU-ENG-84-4002

For Research Supported by

AFOSR Grant No. 83-0041

for period 2/1/83 to 1/30/84

-entitled-

A PLASMA INITIATION/FLOW CHAMBER TO STUDY CW LASER BEAMED ENERGY ABSORPTION IN LIGHT GASES

prepared by

Herman Krier[1] and Jyoti Mazumder[1]
Ronald J. Glumb[2], Terrence D. Bender[3], and Todd J. Rockstroh[3]

Department of Mechanical and Industrial Engineering
University of Illinois at Urbana-Champaign
144 MEB, 1206 W. Green St., Urbana, IL 61801

work supported by

Air Force Office of Scientific Research/NA
Dr. Leonard H. Caveny, Program Manager

(1) Co-Principal Investigators
(2) ONR Fellow
(3) Graduate Research Assistants

APPROVED FOR PUBLIC RELEASE;
DISTRIBUTION UNLIMITED

Abstract

This report summarizes the research work that has been done in the past year, investigating the use of laser-sustained plasmas for propulsion applications. One focus of the research is the initiation of plasmas in inert gases using metal targets and metal vapor seedants. Another is to define the operating characteristics of the dual-flow design by measuring temperatures, number densities, and global absorption. A pressure chamber has been built to permit observations of the plasma under wide ranges of pressure, flow conditions, and beam geometry. Laser energy absorption will be measured using a high-flux calorimeter, and temperature profiles will be found using a combination of spectroscopic relative line intensity measurements, thermocouples, infrared thermography, and possible laser induced fluorescence. The report summarizes the design and construction of the pressure chamber, optics, and related equipment, and discusses the techniques which will be used to analyze temperatures throughout the flowfield.

Table of Contents

I) Introduction

During the past decade, interest has steadily grown in the idea of using high energy lasers for beamed energy propulsion applications. Such a scheme has an important potential advantage over existing propulsive systems: the ability to produce moderate levels of thrust at high specific impulse. Such a system could bridge the gap between high-thrust, low specific impulse chemical systems, and high specific impulse, low-thrust electric propulsion.

The eventual goal of ongoing CW research is to investigate the feasibility of using the CW process for the efficient, and economical, production of thrust in space. To be an attractive alternative to existing propulsive systems, a laser thruster must be capable of producing thrust in the thousands of newtons, at a specific impulse in excess of one thousand seconds, while operating at an overall thermal efficiency near fifty percent. To accomplish this, the thruster must be capable of high internal temperature (to produce high specific impulse), steady flow, strong absorption, and low heat losses. To date, the feasibility of each of these requirements is unknown.

There are two distinct types of CW operation currently being investigated: the dual flow plasma design and direct heating of the propellant through molecular seedant absorption. Although these two branches are closely related, the work at the University of Illinois concentrates on the first type; namely, studying high temperature plasmas in a dual-flow hydrogen environment. A schematic summary of the physical processes operating in such a device is presented in Figure 1. Specific questions that need to be answered include the following. Can stable plasmas be created in flowing pressurized inert gases (especially hydrogen)? What techniques can be used to ensure reliable plasma initiation? What percentage of the incident laser energy will be absorbed? What are

FIGURE 1

PHYSICS OF BEAMED ENERGY PLASMA HEATING

UNIVERSITY OF ILLINOIS AT URBANA-CHAMPAIGN

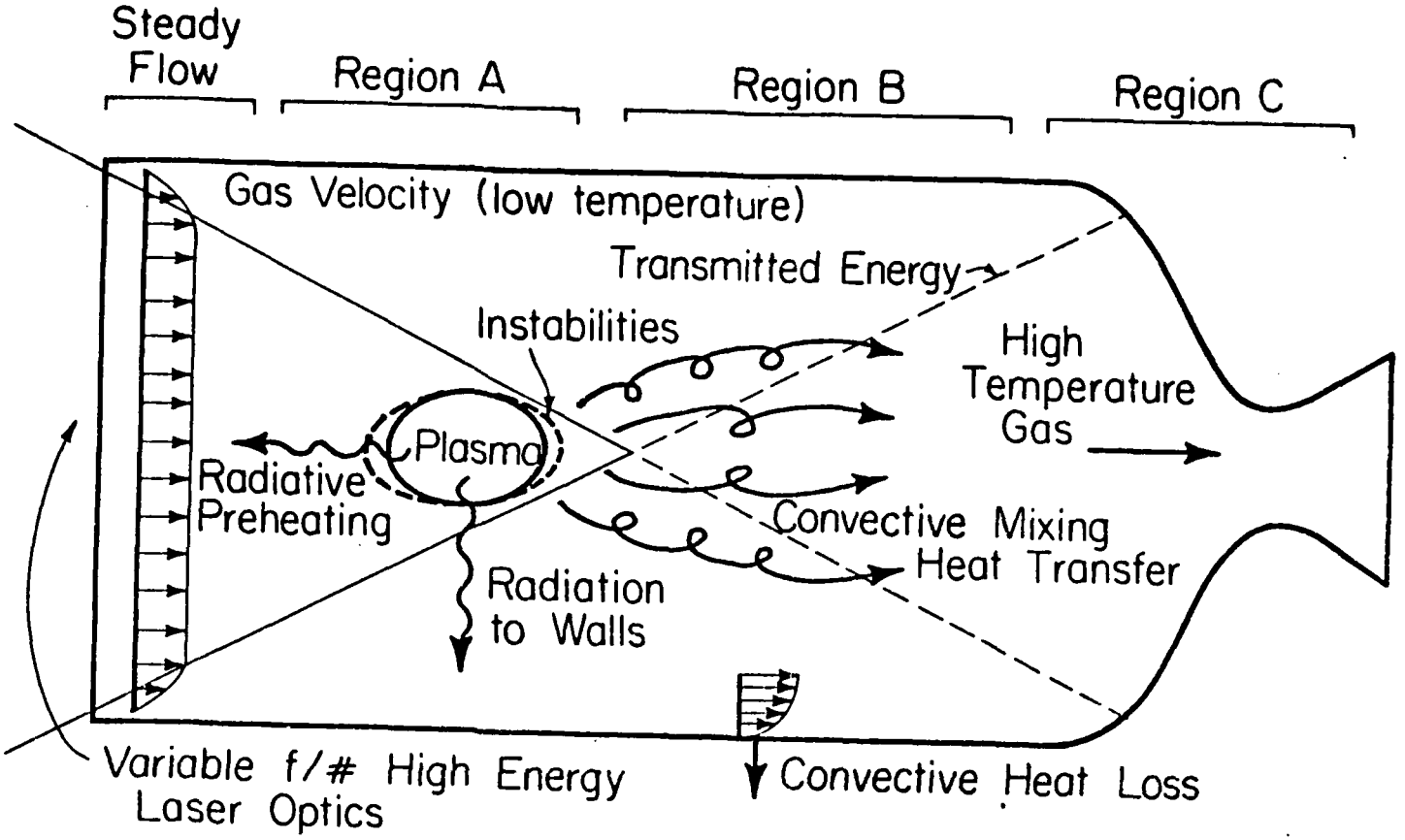

- *HIGH-TEMPERATURE PLASMA IS HELD STATIONARY IN A CONVERGING BEAM.*
- PLASMA PROPAGATION VELOCITY (A FUNCTION OF INTENSITY) JUST MATCHES THE FLOW VELOCITY AT THE DESIRED PLASMA LOCATION.

  PLASMA IS INITIATED BY SUDDENLY CREATING A CASCADE OF FREE ELECTRONS AT THE FOCUS (USING TARGETS, SEEDANTS, OR A PULSED LASER).
- PLASMA MAY EXHIBIT HIGH-FREQUENCY OSCILLATIONS AND ABSORPTION INSTABILITIES.
- BEHAVIOR DEPENDS ON FLOW VELOCITY, PRESSURE, F/# OF OPTICS, ETC.
- IN REGION A:
  - HIGH-TEMPERATURE TURBULENT LOW-Re FREE CONVECTIVE FLOW REGIME
  - HUGE DENSITY GRADIENTS AND SIGNIFICANT BUOYANCY EFFECTS
  - UPSTREAM RADIATIVE PREHEAT ZONE
  - COMPLEX LOCAL ABSORPTION BEHAVIOR
  - VERY HIGH LEVELS OF RADIATIVE HEAT TRANSFER TO WALLS
- IN REGION B:
  - MODERATE-TEMPERATURE MIXED FREE/FORCED CONVECTIVE FLOW REGIME
  - TURBULENT UNSTEADY SHEAR LAYER MIXING ZONE
  - LIMITED ABSORPTION OF TRANSMITTED LASER ENERGY
  - LIMITED ADDITIONAL HEATING DUE TO RADIATION FROM PLASMA
  - CONVECTIVE HEAT LOSSES TO WALLS
- IN REGION C:
  - EXHAUST GASES MAY NOT BE THOROUGHLY MIXED (HOT SPOTS AND INSTABILITIES)
  - EXHAUST GASES MAY NOT BE IN VIBRATIONAL/ROTATIONAL EQUILIBRIUM (INEFFICIENT THRUST PRODUCTION)
  - TRANSMITTED LASER ENERGY CAN BE MEASURED USING A CALORIMETER
- PEAK TEMPERATURES, PLASMA STABILITY, EASE OF INITIATION, AND OVERALL EFFICIENCY MAY BE MODIFIED BY USING SEEDANTS.

the peak temperatures within the plasma core and the bulk temperatures downstream at the nozzle entrance? How does the flow behave during the crucial mixing of the hot and cold gas flows? And, most importantly, what are the heat losses to the chamber walls and what is the overall efficiency of the thruster?

This report summarizes the efforts made in the past year to answer many of these questions. Section II contains a brief history of the results of past investigators, followed by a discussion of the specific goals of our research work. Sections III and IV describe the experimental equipment and procedures in more detail, and Section V summarizes the work that has been accomplished to date and presents a schedule of future activity.

II) Scientific Objectives

Work on CW type thrusters has a fairly long history. One of the first experimental studies in this country was conducted in 1974 by Pirri[1]. In these tests, a quasi-CW laser (actually a "long" 100 microsecond laser pulse) struck solid targets, and the impulse that was produced was measured. Although these tests should truly be regarded as crude RP tests, they did indicate that the production of thrust was somewhat efficient. It was also concluded that a more stable method of heating the propellant was needed.

It was soon recognized that a stationary plasma could be used as the source of such stable heating. Laser-sustained air plasmas have been studied by physicists for some time, especially in the Soviet Union, and a thorough experimental study of these plasmas was made by Fowler in 1975[2]. Using a 15 kW CW CO_2 focused laser, Fowler first measured initial wave speeds of the plasma, as well as the laser intensities required to ignite and sustain the plasmas. It was found that maintenance intensities had a curious inverse square dependence on beam diameter, indicating that the required minimum intensities fell rapidly as the focal spot size increased. It was also found that the plasmas tended to be stable phenomena, as long as the focal number of the focusing optics was less than ten. Typically, the plasma would be ignited at the focus point, and would then begin propagating back up the converging beam until it reached a location where the laser intensity matched the intensity required to sustain the plasma. Another finding was that roughly half of the laser energy passed through the plasma without being absorbed. Finally, Fowler made use of a laser interferometer to obtain accurate 2-D temperature and number density profiles of the stationary air plasmas. Results indicated peak temperatures just over

16,000K, and showed a roughly cylindrical plasma 0.5 cm in diameter and two centimeters in length. The tests were all conducted in stationary atmospheric pressure air.

At nearly the same time, Henricksen and Keefer[3] were conducting similar experiments in air using a 6 kW CW laser focused through a 15 cm focal length NaCl lens. A spark gap was used to ignite the plasma. The plasma was found to be of roughly the same size as in Fowler's tests, except that they observed a lower temperature region behind the plasma that extended some 30 cm downstream. Detailed 2-D temperature profiles were made using spectroscopic analysis of continuum radiation. No calibration source was used; instead, the calculated emission peak was fitted to the peak isotherm and the other temperatures were evaluated relative to that value. The result showed peak temperatures of just over 17,000K, and maintenance intensities of 120 kW/cm^2 were reported.

It has not been until very recently that experimental work has been extended to hydrogen plamas by Fowler[4], who studied laser-sustained plasmas in hydrogen and in hydrogen/seed mixtures specifically for propulsion applications. The focus of this work was to measure the absorption coefficient of the various mixtures as a function of temperature. The effect of adding a seedant is to dramatically increase the absorption coefficient at low temperatures, and in general this results in a lower temperature plasma.

Fowler used a 7 kW CW CO_2 laser, focused by a 1 cm focal length mirror into a small high pressure cell (maximum pressure of 5 atm). The beam entered through a single zinc selenide window, which had to be moved back several centimeters farther from the focal point when it was found that convection from the plasma caused the window to crack repeatedly. Unlike what we plan to do, as

will be discussed shortly, the beam entered the chamber vertically downward, allowing the heated gas to be convected up to the window. We plan to introduce the beam vertically upward, so this should not be a problem. Nearly all previous investigators have used vertically introduced beams so as to produce symmetrical plasmas that are not radially affected by gravity and buoyancy forces.

In the Fowler experiments, temperature and absorption coefficients were measured simultaneously by passing a diagnostic laser interferometer through the plasma. Results show a significant rise in absorption, compared to pure hydrogen, at temperatures up to about 5000K, at which point the seed molecules (H_2O,-D_2O,NH_4) began dissociating, causing absorption to drop sharply. In most of these tests, Fowler used a low power pulsed laser to ignite a low temperature plasma, but he also made an important finding. When seeded, the gas could be heated directly (up to about 3000K) without the formation of a plasma. Maximum temperatures were thus fairly low, but the heating process was direct and was found to be stable, suggesting it could be used to avoid the high temperatures and heat losses inherent in a thruster using a plasma.

Soon after Fowler's tests, Kemp [5] suggested that heat losses in such a direct heat addition thruster could be an order of magnitude higher than for a comparable dual-flow plasma device. This was because the direct heat thruster would have to allow the hot flow to entirely fill the chamber, whereas the dual-flow device uses a cold buffer flow to reduce heat losses. After this finding, attention seems to have shifted back to the pure hydrogen dual-flow scheme.

Interest in this scheme was further raised when in 1979 Conrad and Roy[6] were successful in creating stationary plasmas in flowing hydrogen gas. Using a 30 kW CW laser, they showed that initiation occurred at intensities an order of

magnitude lower than had been predicted (actual values near $3x10^5$ W/cm^2), and that the absorption process was in general stable. Funding limitations prevented further study of the plasmas.

This situation changed when the 30 KW laser was transferred to NASA-Marshall, where Jones, McCay and co-workers[7] began a program designed to study hydrogen plasmas in more detail. The goals of the research are straightforward: to investigate the plasma initiation process and measure temperatures within the plasma region.

The experimental set-up consists of a cylindrical chamber (13 cm ID) into which the laser is focused using a sodium chloride lens. The chamber contains pure hydrogen at pressures up to five atmospheres. Plasma initiation is produced using a 6J 100-nanosecond pulsed CO_2 laser, cofocused through the primary NaCl optics. One priority of the work is to produce detailed studies, using high speed photography, of how the pulsed laser causes breakdown, and at what intensity levels this breakdown occurs. Another goal is to measure two-dimensional temperature distributions inside the plasma core. This is accomplished by digitally analyzing the output of a video camera, and using the absolute intensity of continuum radiation to determine electron temperature.

Similar work is just getting underway at the University of Tennessee by Keefer. Using a 1.5 kW CO_2 laser focused into a small diameter quartz tube, he expects to study in detail the flow and heating behavior of the plasma core region. A small diameter is used so that the actual convective flow in the core can be closely observed. Quartz is used because it transmits much of the plasma radiation, and will withstand the high temperatures encountered near the plasma. The rear of the chamber is equipped with a calorimeter, and temperature data is obtained using digital image processing. One limitation to using a

To get an optimum view of the plasma, the viewing windows have been placed on either side of the chamber, and offset slightly. One window is located so that its center is at the laser focus point; the second window is centered 1.75 inches downstream. Both windows are 6.75 inches (17.15 cm) high, 3.0 inches (6.99 cm) wide, and 0.5 inches thick.

Details of the viewing window assemblies are shown in Figure 6. First, a flange is nickel-brazed to the chamber, then an inner plate is bolted onto the flange. This plate is recessed to hold the viewing window and comes with a machined slot for an O-ring seal. The size of both the flange and the inner plate are 10.0 by 6.25 inches, and they are held together using bolts that are recessed into the inner plate. A tight seal is achieved using a liquid type gasket that is applied and allowed to cure. The inner plate currently is designed to hold a one-half inch thick piece of tempered Pyrex. According to the manufacturer, this thickness is adequate for chamber pressures up to ten atmospheres as long as the window temperature remains below 500K. The final item is a cover plate that holds the Pyrex window in place. This plate also has provision for an O-ring seal, and is attached to the inner plate using fourteen three-eighth inch bolts.

There are several reasons why this somewhat complicated window arrangement has been used. Since we do not yet know what the window temperature will be under operating conditions, it is possible that one-half inch thickness is inadequate. For this reason, the inner plate, which holds the window, is removable and can be replaced with a plate that can hold a thicker piece of Pyrex. As an alternative, the inner plate can be redesigned to incorporate a support bar that divides the window area in half and gives the window more structural support. In either case, the inner plate can easily be removed and replaced without cutting and rebrazing.

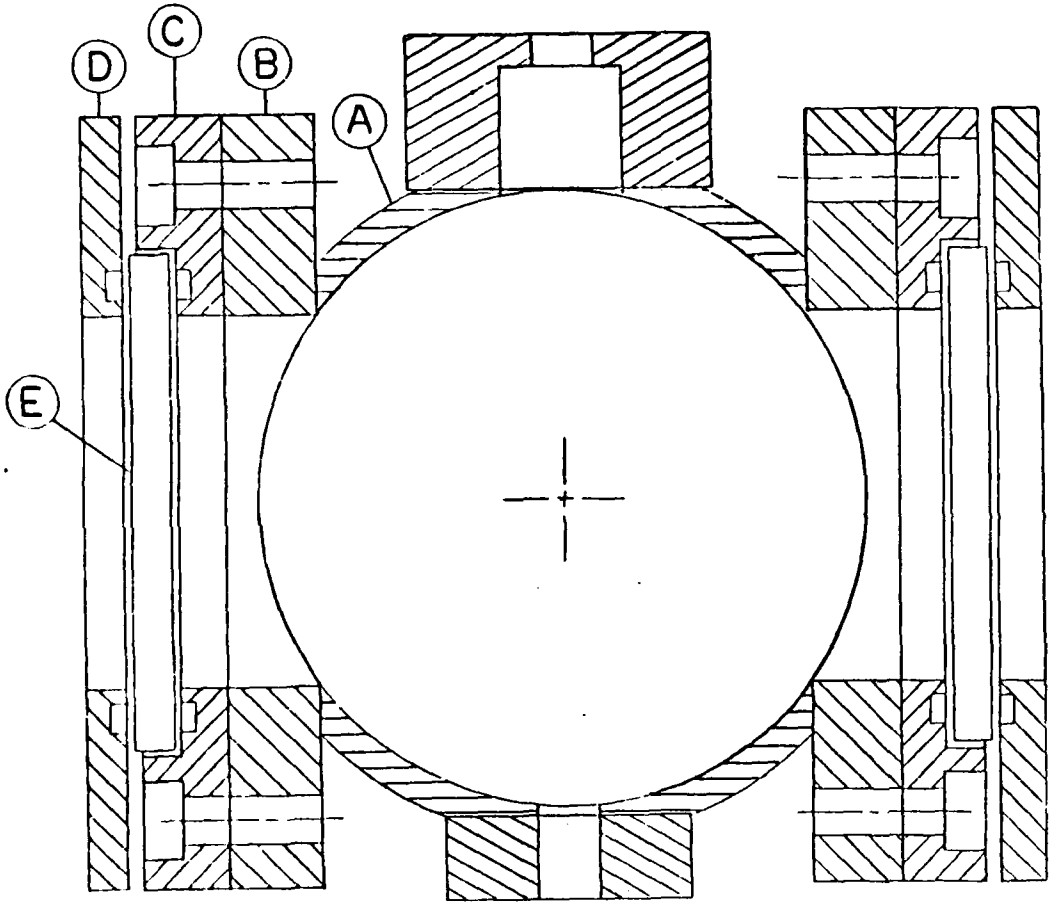

(A) Chamber Wall
(B) Viewing Window Flange
(C) Inner Plate
(D) Window Cover Plate
(E) Viewing Window

Figure 6 Viewing Window Design

windows. Any laser energy not absorbed by the plasma is collected by the calorimeter. Other major parts that have been added to the chamber include a target/air cylinder assembly, a pressure transducer, a pressure rupture disk, and a moveable thermocouple assembly (located inside the chamber) with a wire lead collecting box and stepper drive motor.

The main chamber section is constructed of Type 304 stainless steel, one-quarter inch thick, five inches ID, and fourteen inches long from the rear flange to the gas inlet assembly. Stainless steel was chosen for its high temperature strength and for its corrosion resistance, a property that may become important if corrosive seedants are ever used. The chamber walls are 0.25 inches thick to assure a large structural safety factor, and to provide adequately large brazing surfaces for all fixed attachments, especially the viewing windows. The top of the chamber is a simple 9.25 inch (23.5 cm) diameter flange, which supports the bolt-on calorimeter (discussed later), and the bottom end attaches to the gas inlet assembly.

The design of the two viewing windows has been given a great deal of consideration, and the final design detail is shown in Figure 6. When designing the windows, several factors had to be considered. First, the windows need to be as large as practical in order to permit diagnostic viewing of both the plasma and as large a downstream area as possible. They also have to be located so as to cover a wide area on either side of the focus point, in case the optics do not place the plasma in the desired spot. Finally, the actual window material must be strong enough to contain the design pressures while being transparent to the bands of radiation which are emitted by the plasma and which can be used for spectroscopic analysis.

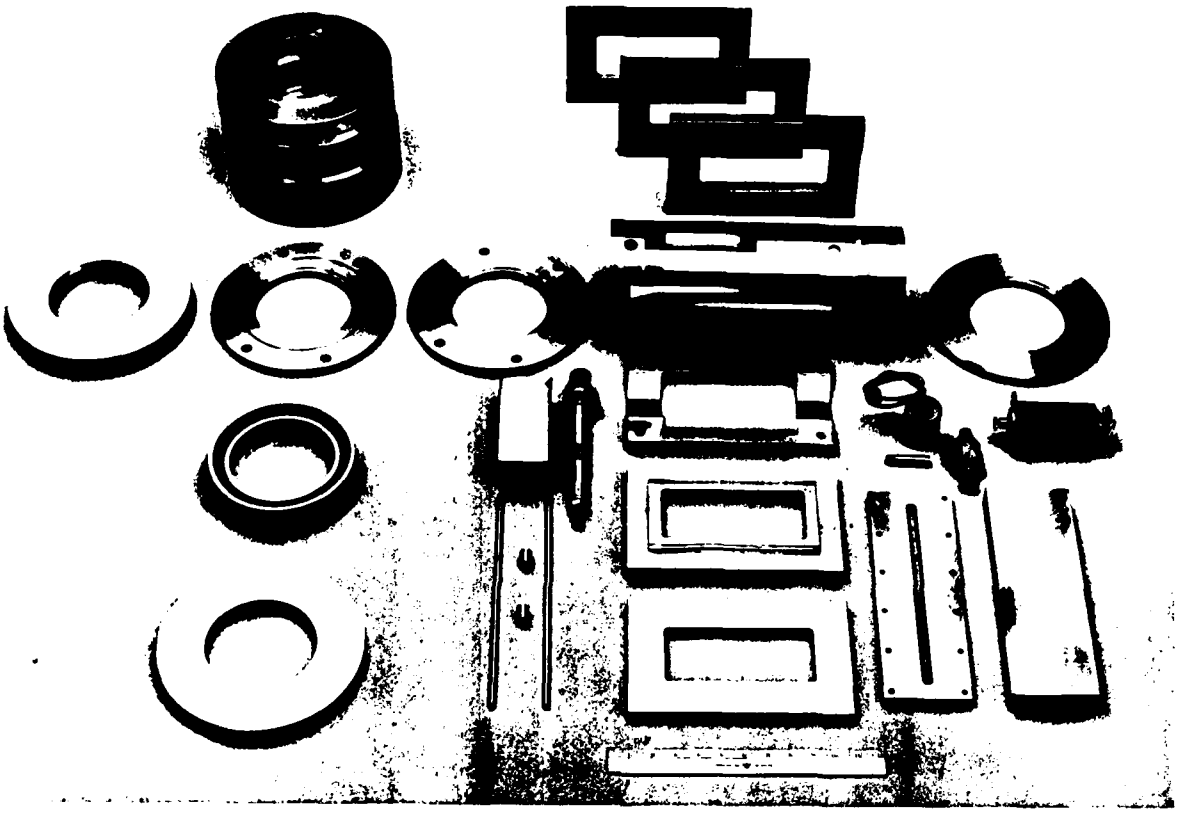

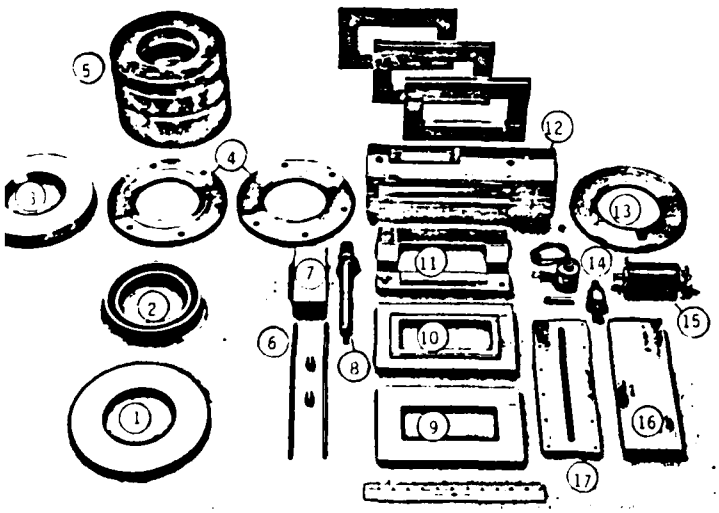

1) Inlet Section Flange
2) Gas Inlet Assembly
3) NaCl Window Cover Plate
4) Flanges
5) Chamber Extension Plates
6) Linear Bearings and Rails
7) Air Cylinder Flange
8) Air Cylinder
9) Viewing Window Cover Plate
10) Viewing Window Inner Plate
11) Viewing Window Flange
12) Main Chamber Section
13) Flange to Calorimeter
14) Pressure Transducer and Relief Valve
15) Thermocouple Carriage Drive Motor
16) TC Wire Retract Box Flange
17) TC Wire Retract Box Mount

Figure 5 Experimental Flow Chamber - Exploded

(A) Laser Inlet Window Assembly
(B) Gas Inlet Assembly
(C) One-Half Inch Inlet Pipes (2)
(D) Main Chamber Section
(E) Thermocouple Wire Retract Box
(F) Viewing Windows (2)
(G) Target / Solenoid Assembly
(H) Pressure Transducer and Popoff Valve
(I) One-Half Inch Exhaust Pipes (4)
(J) Thermocouple Drive Motor
(K) Calorimeter
(L) Laser Inlet Window

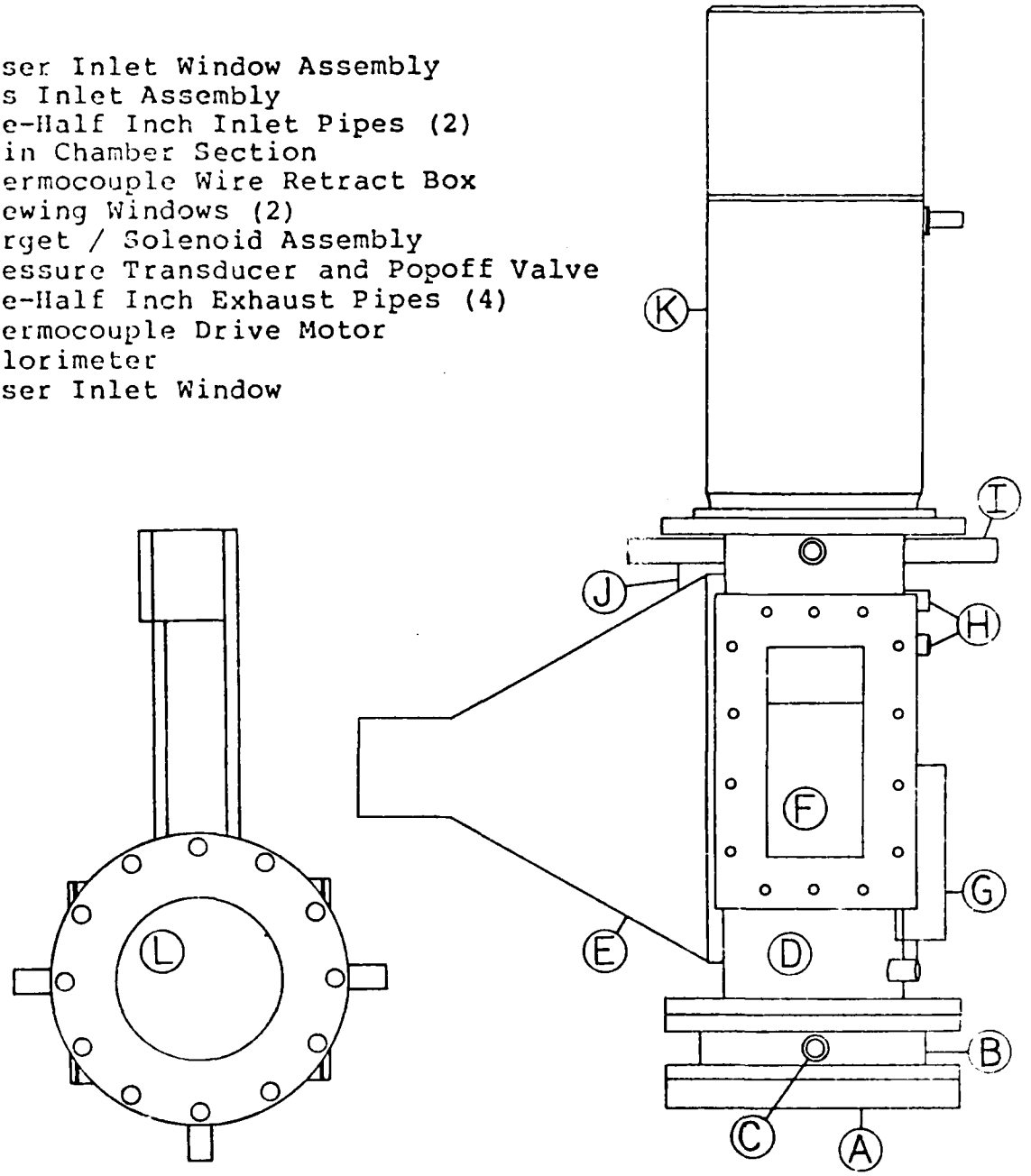

Figure 4 Experimental Flow Chamber - Schematic

III) Experimental Equipment

Initiating and maintaining plasmas in pressurized gases and diagnosing the properties of these plasmas requires the use of specialized pieces of equipment. This section summarizes some of the more important items, explaining their purpose and construction.

A) Pressure Chamber

Containing the high pressure environment is of course crucial, and to do this, it is necessary to build a pressure chamber. In general, the chamber must be rugged and capable of withstanding internal pressures up to 150 psia, must not allow any gas leakage, and must allow for a uniform steady flow of gas. In addition, there must be adequate provision for chamber windows, both for laser access and for viewing the plasma. There must also be thermocouples located inside the chamber to measure gas temperatures at various points in the flow. Finally, the chamber must incorporate a calorimeter to monitor the percentage of laser energy that is transmitted by the plasma.

The overall design of the chamber that has been selected to meet all these requirements is shown in Figure 4. The major components of the chamber are (from bottom to top) the laser inlet window assembly, the gas inlet assembly, the main chamber section with viewing windows and gas exhausts, and the top-mounted calorimeter. Figure 5 is an exploded photograph showing the disassembled components of the chamber. The overall chamber is eighteen inches (45.72 cm) long with a five inch (12.7 cm) ID, and the calorimeter adds an additional fifteen inches (30.1 cm) in length. The laser enters the chamber from the bottom through the laser inlet window and is focused by external optics to the focus point, where a plasma is formed and observed through the two viewing

tion coefficient in the plasma and downstream. Such measurements are useful in understanding laser coupling within the plasma, and could be a valuable method of independently checking plasma temperatures and global absorption.

Another interesting addition to the schedule of experiments would be to study the effect of gaseous seedant injection into hydrogen flows. The purpose would be to look for changes in peak and bulk temperatures, overall absorption, plasma stability, and to study seedant breakdown.

Finally, it is possible, with little modification, to surround the chamber with a hollow outer wall, in effect creating a water-cooled sidewall calorimeter. It would thus be possible to measure exactly how much energy is being lost to the chamber walls. These measurements could then be compared to the estimates obtained earlier.

In the sections that follow, the experimental procedures and equipment are described in more detail. Section III discusses the pressure chamber and the test stand, including details of construction and operation. Section IV is a summary of high-temperature gas diagnostics, and presents the equipment and procedures we will be using to analyze the plasma core and the high-temperature downstream mixing zone. The final section summarizes our progress to date and presents a tentative schedule for work in the second year of this program.

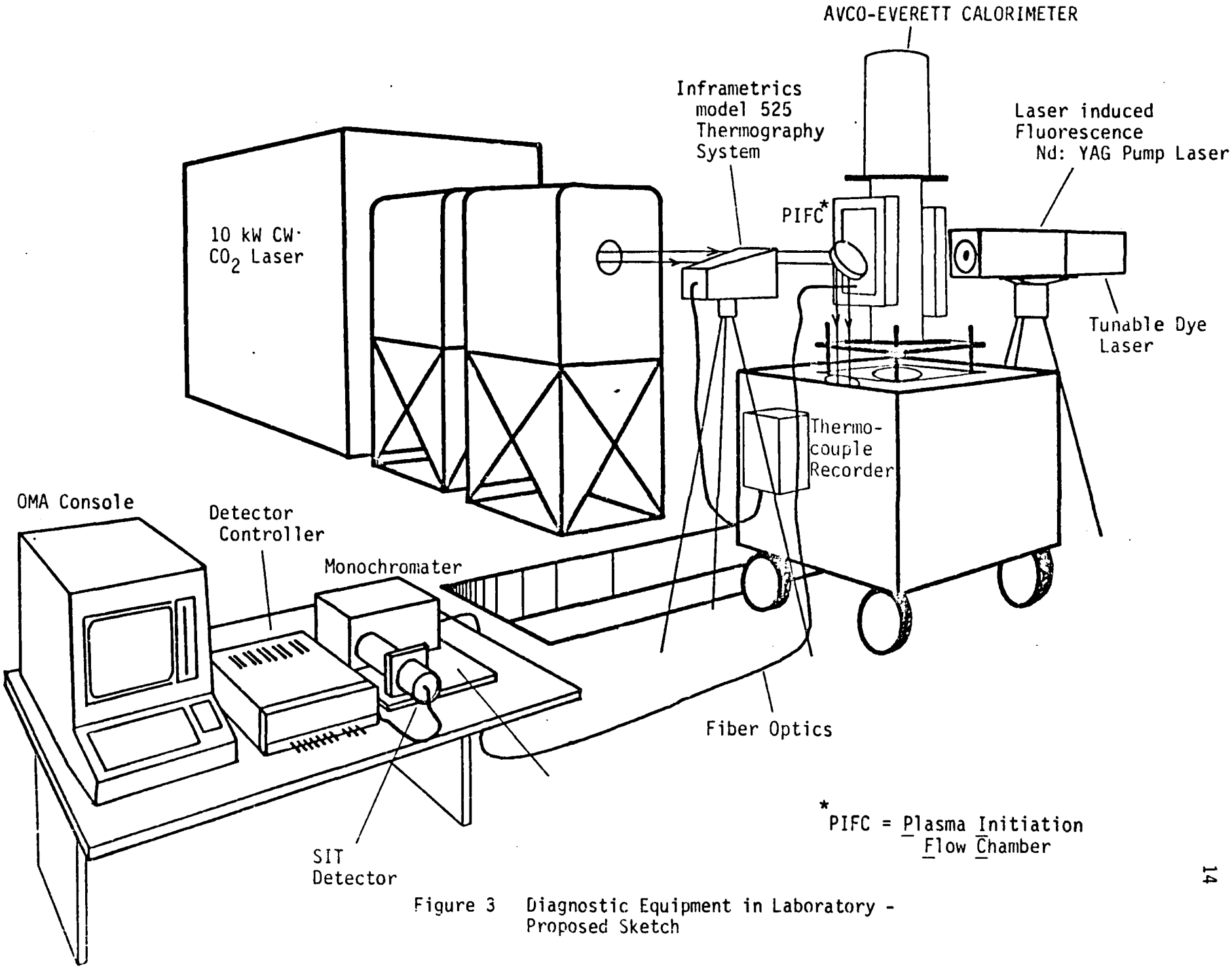

Figure 3 Diagnostic Equipment in Laboratory - Proposed Sketch

stream flow. Examining this flow is difficult, since most of the mixing takes place in the temperature range 2000-10,000K, where spectral lines tend to be quite weak. Towards the lower end of this range (under 3200K), it is our intention to construct three-dimensional temperature profiles of the downstream flow using a moveable grid of high-temperature thermocouples. Themocouples will also be used to monitor wall and bulk exit temperatures.

Above 3200K, other techniques are needed. In argon, spectroscopic temperature resolution down to about 4000K is possible, so there is only a small data gap. In hydrogen, where no resolvable transitions exist, we will attempt to use two independent techniques. First, an infrared thermography system sensitive to radiation emitted in the range 8-12 μm will produce video scans of the downstream region. Due to uncertainties in emissivities, data analysis will be difficult, but this method should give considerable qualitative information on mixing.

A second technique is laser-induced fluorescence (LIF), a procedure in which a low power tunable dye laser is directed into the gas to induce emittance at a desired wavelength. The gas emission can be analyzed (using the OMA system) to produce downstream temperature profiles. LIF is a proven method of flow visualization in combustion studies. Typically, a seedant is introduced into the flow, and its emissions are used for analysis. It remains to be seen if a suitable candidate can be found for the temperature range of interest. Figure 3 is a sketch of the diagnostic and test equipment that we plan to use, shown assembled in the laser laboratory.

Further in the future, once the initial phase of the experimental work has been completed, other aspects of the CW process may be studied. One possibility is to use a tunable dye laser (from the LIF system) to measure the gas absorp-

wall temperature readings, the calorimeter data should provide reasonable estimates of wall heat loads and overall thermal efficiency.

Of course, the major emphasis of our ongoing research is the study of the plasma core region; specifically, the development of accurate three dimensional steady state profiles of electron temperature, ion temperature, and electron number density. These will be produced using an EG&G optical multichannel analyzer (OMA), a system used to scan and analyze the spectral lines of emitted plasma radiation. In hydrogen, we will be analyzing Stark broadened H-beta lines for number density, Doppler broadening for ion temperature (if resolvable), and relative line-to-continuum intensities for electron temperature. These techniques are only reliable down to about 12,000K, but by injecting a doubly-ionizable seed and analyzing two-line relative intensities, this range may be extended down to about 10,000K. In argon, we will analyze the relative intensities of three pairs of emission lines to measure electron temperature in the complete range from 3000 - 15,000 K. Number density will be measured using absolute intensity techniques.

Temperature measurements of the core can also be used to qualitatively assess the size and shape of the plasma region, and it may be interesting to observe what effect different beam geometries has on plasma shape. The OMA system can also be used to analyze the spectral intensity of thermal radiation emitted by the plasma, data which could be useful in modeling radiative loss mechanisms.

Equally important to the operation of the dual-flow process is the mixing behavior of the hot and cold flows, and how this behavior changes with flow velocity and beam geometry. One of the prime considerations in the design of the chamber was to permit complete and undisturbed observations of the down-

The actual initiation of the plasma will be caused by focusing the laser onto a small retractable metal target, creating a cascade of electrons. Target candidates include Group I materials (such as cesium) due to their relatively low ionization potentials (< 6 eV). The first objective is to measure breakdown intensities for the different metals under various operating conditions; measuring, for example, the dependence of breakdown intensity on flow velocity, gas pressure, laser power, and F number. Spot sizes will be measured using a photon drag detector system. Another early goal is to attempt initiation without the use of a target or any external source. Instead, by using a small focal spot size and metal vapor seedants in the flow, it may be possible to directly cause initiation. In either case, it would be useful to measure breakdown intensity as a function of seedant concentration. The eventual goal of these studies is to find a simple, yet highly reliable method of plasma initiation.

Once reliable plasma initiation has been achieved, the next step will be to assess the stability of the plasmas, and to see under what conditions instabilities and oscillations occur. Chamber pressure, flow velocity, flow pattern, beam geometry, and laser power may all be used as variables.

Having established stable plasmas, the next priority is the study of global laser energy absorption, using a high-flux calorimeter attached to the rear of the pressure chamber. This instrument measures the overall percentage of laser energy that is absorbed by the gas. The purpose here is to find conditions for maximizing absorption and minimizing absorption lengths. The main variable will be gas pressure, but the effect of mass flow rate, laser geometry, and seed concentration will also be examined. In addition, an attempt will be made to define any correlations between overall absorption and bulk downstream temperatures, as well as with peak plasma core temperatures. Together with exit and

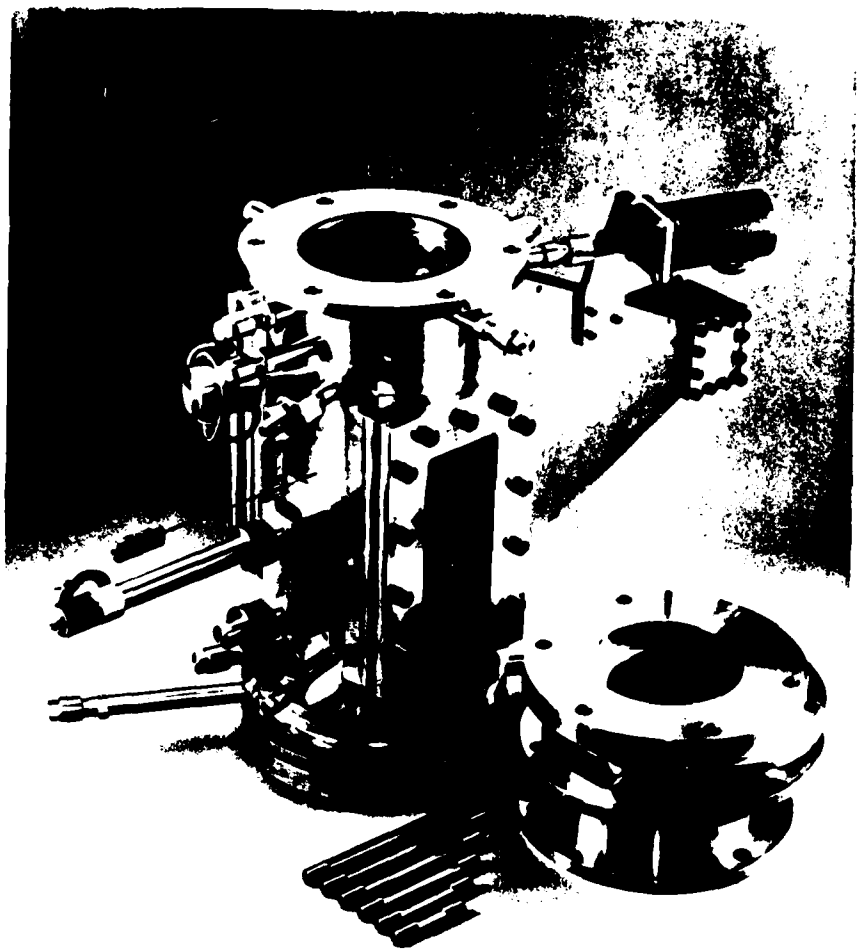

Figure 2 Plasma Initiation Flow Chamber

process by examining the operating characteristics and overall performance of an experimental flow chamber (shown in Figure 2).

The first important goal is the initiation and stable maintenance of plasmas in selected gases. The plasmas will be created under steady flow conditions in a pressurized stainless steel chamber. The chamber uses a relatively large five inch inner diameter so that flow mixing can be thoroughly observed without interference from wall effects. A converging 10 kW CW CO_2 laser beam is focused into the chamber using a variable f number optical system, and enters vertically upward through a sodium chloride window.

Perhaps the most important decision yet to be finalized concerns the choice of gas to be used in the flow experiments. As mentioned earlier, hydrogen is the preferred choice, both because it is the best potential propellant and because little is known about its behavior in laser-sustained plasmas. However, due to the safety problems related to the use of hydrogen, a substitute must be used to calibrate our diagnostic equipment while a hydrogen safety system is being devised.

At this time, the best choice appears to be argon. To begin with, the physical behavior of this gas should be nearly identical to that of hydrogen, and the resultant plasmas should be similar. In addition, argon has the advantage of having a very diagnosable spectrum, and as will be discussed later, it should be possible to produce continuous temperature readings in the complete range from 3000-15,000K. Argon can also be seeded with trace hydrogen to allow analysis at higher temperatures and to permit familiarization with Balmer line techniques. For these reasons, argon has been selected for the initial experimental stages. In the discussion that follows, the procedures mentioned assume the interchangeable use of either hydrogen or argon.

small diameter chamber is that much of the mixing behavior in a dual-flow device cannot be properly studied.

Despite this recent progress, a great deal remains to be done before the physical processes taking place within CW devices can be fully characterized. The most immediate goal is a complete spectroscopic survey of the laser-sustained plasma core. Accurate two-dimensional temperature profiles are crucial in understanding absorption behavior, radiation loss mechanisms, and flow characteristics of the plasmas. In addition to temperature data, measurements of electron density and local absorption coefficient would be highly valuable. Another area of interest is the plasma initiation process. There is a need to define the physical processes that are important in initiation, to measure the laser intensities required for breakdown, and to evaluate the role of seedants in lowering these thresholds.

In addition to studies of the plasma core, there is a need to examine the behavior of the flowing buffer gas and the downstream mixing process. What is needed is a complete three-dimensional temperature map of the entire downstream flow region, to be used to analyze the fluid mechanics of the mixing zone and to maximize the efficiency of the process. Also needed are measurements of global laser absorption and total heat losses to the chamber walls, both of which allow an estimate of global thermal efficiency. Finally, further attention needs to be given to the use of gaseous seedants in hydrogen. Such mixtures are designed to enhance low temperature absorption and could allow direct laser heating without the formation of a high temperature plasma.

The purpose of experiments now underway at the University of Illinois (research funded by AFOSR under grant number 83-0041) is to answer many of these important questions. In general, we hope to judge the feasibility of the CW

The final integral part of the main chamber section is the exhaust section. This consists of four radially placed three-eighths inch ID stainless steel pipes. The only requirement of the exhaust is to allow the heated gas to escape without disturbing the upstream flow, and without allowing any of the not high pressure gas to leak. One of the exhaust pipes is equipped with a thermocouple to allow bulk exit temperature measurements. The four pipes, after leaving the chamber, are rejoined at a four-way connector, then routed through an external stack.

Gas Inlet and Laser Inlet Window Assemblies

Upstream of the main chamber section is the gas inlet assembly, a component designed to inject a pressurized gas into the chamber as a low velocity steady flow. As shown in Figure 7, this section consists basically of two annular rings of stainless steel, held together by a flange at either end. The gap between the two rings is one inch (2.54 cm) and is filled with gas that enters the space through a pair of high pressure gas lines.

To allow the gas to enter the chamber itself, the inner ring has been drilled with a large number of small holes evenly spaced around the ring circumference, shown more clearly in Figure 8. There are, in fact, three groups of holes. One group is angled downstream at a forty-five degree angle, one group is directed radially inward, and the rest are angled forty-five degrees upstream. This last group of holes is used to direct a portion of the flow onto the laser inlet window, which will tend to get hot during operation and will require active cooling. There are eight holes in each group, and this design allows us to tailor the inlet flow simply by plugging up selected holes or by drilling new ones. In addition, a thin ring may be placed over the inlet holes to induce swirl in the flow, if desired.

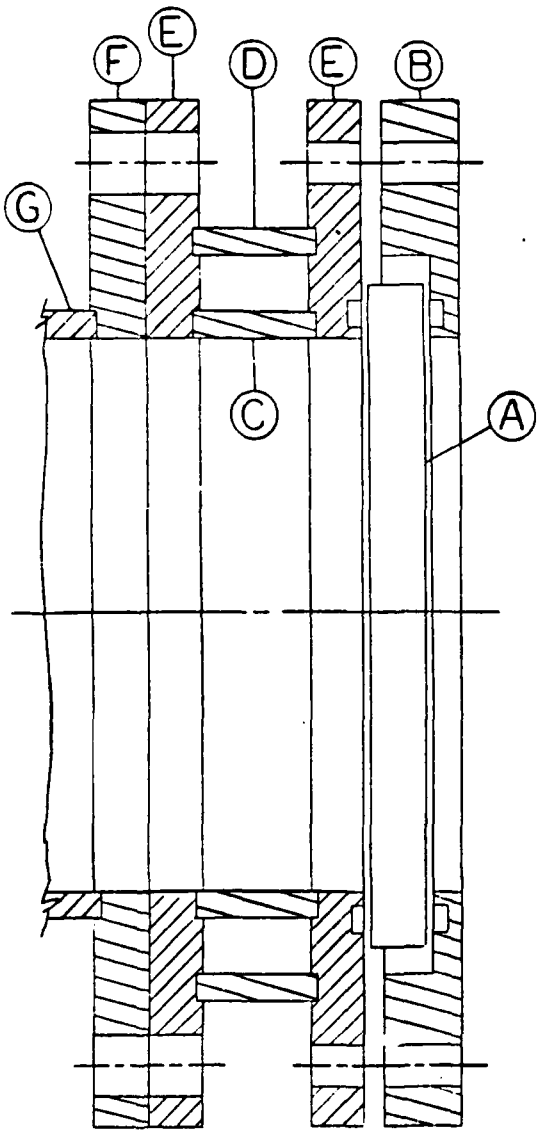

(A) NaCl Laser Inlet Window
(B) Window Cover Plate
(C) Inlet Plenum - Inner Wall
(D) Inlet Plenum - Outer Wall
(E) Inlet Assembly Flanges
(F) Main Chamber Section Flanges
(G) Main Chamber Section

Figure 7 Gas Inlet and Laser Access Window Assembly

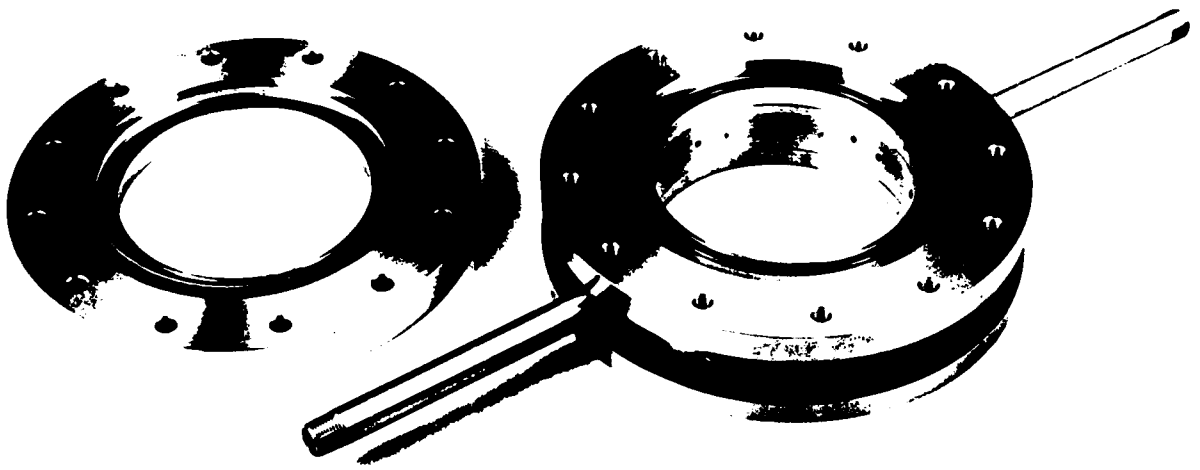

Figure 8 Gas Inlet and Laser Access Window Assembly

The outer ring of the inlet is fitted with a pair of one-half inch ID stainless steel pipes. The pipes are eight inches (15.24 cm) in length, long enough to clear the test stand supports, and are equipped with fittings that attach to laboratory gas lines. Two inlet pipes are used to ensure an equal supply of gas to all the inlet holes, and to ensure that flow oscillations do not occur.

The chamber is bolted atop the inlet section which doubles as the chamber support on the test stand. It is held in place on the stand using a two-piece collar which bolts around the inlet section (see Figure 9). The overall length of the chamber can be extended using spacers which are inserted between the chamber and the inlet section.

The bottom flange of the inlet attaches to the laser access window assembly, and is fitted with double O-ring seals. Getting the high power laser beam into the sealed chamber is one of the more difficult aspects of chamber design. In general, previous investigators have used solid crystalline materials, such as sodium chloride or galium arsenide. Although these materials are near-perfect transmitters of the laser light, some small fraction of the energy is always absorbed. When very high fluxes are used, this absorption leads to the development of thermal stresses in the window material which can lead to cracking. And, if pressurized gases are present in the chamber, a cracked window may shatter.

Two window materials were examined: salt and zinc selenide. Of these, ZnSe is clearly the better material, having higher structural strength and better transmission of 10.6 micrometer radiation; unfortunately, it is an order of magnitude more expensive. Because of this, sodium chloride has been selected as our window material. NaCl windows do, however, present two problems, the

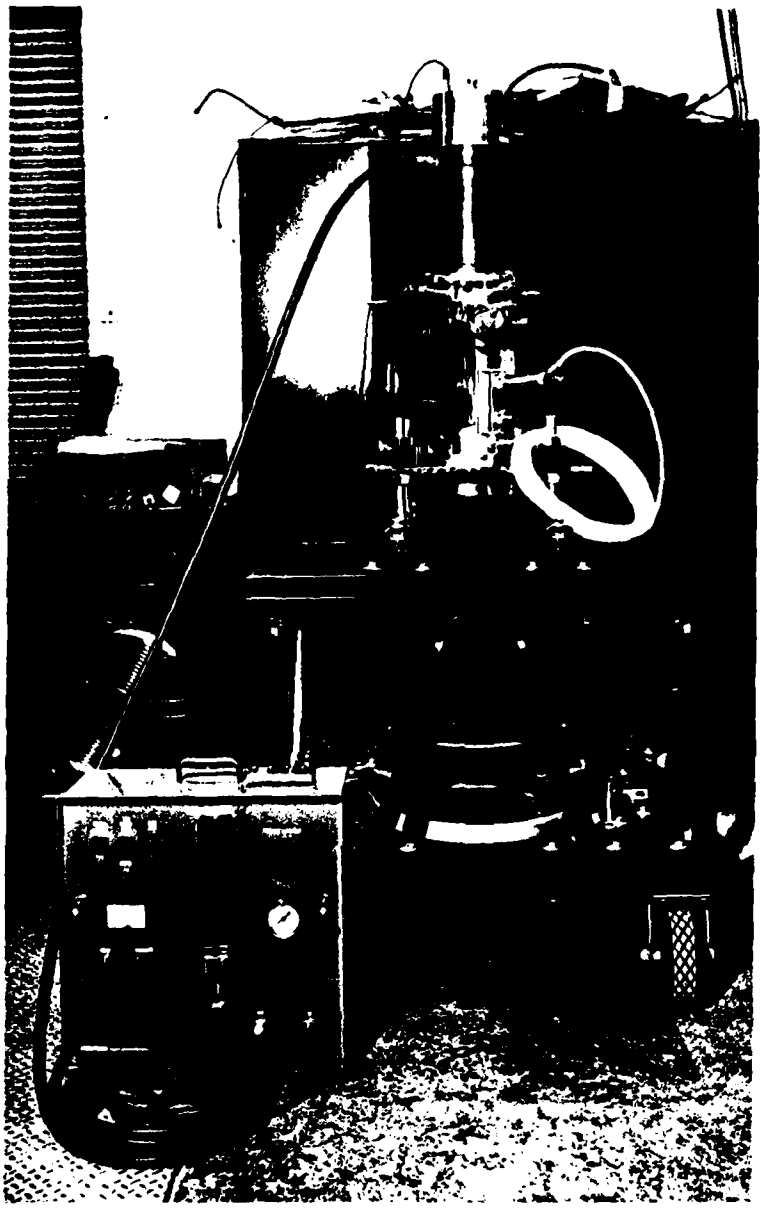

Figure 9 Chamber and High-Flux Calorimeter on Test Stand

minor one being that they are structurally weaker and thus greater thicknesses are required. More importantly, if water or water vapor is ever allowed to come in contact with the NaCl, the result is a puddle of salty water where a $200 window used to be. To avoid this unpleasant situation, it is necessary to keep the window constantly heated to prevent any buildup of water in the salt. When not in use, the windows are stored in an evacuated desiccator. Eventually, if window breakage problems can be reduced or eliminated, ZnSe will be used.

Figure 8 shows the main components of the laser inlet window assembly. The window itself is a six inch diameter, one-half inch thick NaCl crystal, is sealed using two O-rings, and is held in place on one side by the gas inlet flange, and on the other by the laser window cover plate. Although making the window fill the entire five inch diameter of the chamber tends to increase the stresses on the window, it was felt that the larger size would allow us to use lower laser fluxes, ultimately prolonging the life of the window. Note that only five inches of the six inch diameter are actually exposed to the laser beam.

Since we expect to have to replace the window regularly, replacement was made simple. The chamber will be oriented with the laser inlet window down, so replacing a window means simply dropping the cover plate down and installing a new window in the recessed section of the cover.

Another feature of the design is the small gap around the outer edge of the window. A one-half inch wide electric heating strip has been inserted in this space and operated constantly to prevent humidity from attacking the NaCl. This heater also has another purpose. Whenever the laser is first turned on, transient stresses can develop if the window is not first preheated to near its operating temperature. By preheating our window with the heater strip, this thermal shock should be minimized.

Another potential window problem is that, under steady operating conditions, cracking can occur when temperatures within the window exceed a critical value. This possibility can be reduced by cooling the window convectively with a cool jet of crossflowing gas. In our design, both sides of the window are actively cooled; the outside by a flow of cool air, the inside by properly routing some of the cool inlet flow back to the window.

Calorimeter

The final major component of the pressure chamber is the high flux water-cooled calorimeter. This device is used to measure the percentage of the incident laser energy that is transmitted by the plasma, information which is important in estimating heat losses to the chamber walls and in gauging absorption in the gas. The calorimeter is attached to the chamber downstream of the exhaust and is bolted in place on a stainless steel flange.

The calorimeter works by collecting all of the radiation that is either transmitted or scattered by the plasma, as well as any energy that is emitted by the plasma (this quantity should be an order of magnitude smaller). The remaining laser energy is either absorbed by the gas or lost to the chamber walls. Of course, some of the laser energy will also be scattered out the two side viewing windows, as well as backscattered out the laser inlet window, so it will eventually be necessary to measure this loss. In addition, since the calorimeter is mounted above the chamber, heated gases will tend to collect within the calorimeter cone, affecting power readings. This effect will either have to be measured and corrected for, or an additional NaCl window will be needed to isolate the calorimeter.

The calorimeter can be seen bolted to the chamber in Figure 9. It is fifteen inches (38.1 cm) high, seven inches (17.78 cm) in diameter (less its brass mounting flange) and has a collecting diameter of 4.49 inches (11.4 cm), slightly less than the chamber ID of five inches. The water inlet fixture is seen on the side with a water hose attached. The top of the calorimeter contains the cavity at the cone apex, the water outlet fixture, and the thermocouples and electronics needed to measure the inlet and outlet water temperatures. The internal copper cone is surrounded by a lexan housing, and its factory fitted mounting flange was designed for an operating pressure limit of 150 psia. The calorimeter is sealed on the chamber like the other flange mounted fixtures with an easily applied liquid gasket material that provides excellent leak protection.

The calorimeter has been precalibrated by Avco-Everett, the manufacturer, at the factory using an internal heating element of known output to simulate laser power input to the copper cone. The calorimeter has recently been used to measure the laser output without any intervening optics. The data this test provided is being compared to other independent calibration data on the laser itself to estimate its actual power output.

The calorimeter measures the temperature of the water circulated through the absorbing copper cone at the inlet and outlet, and converts this to an electrical signal by means of a standby control module. This signal is amplified and scaled, and can be read from a meter on the control module. The calorimeter has a maximum service limit of 25 kW continuous duty, but by presetting the flow rate to 5 liters per minute, the maximum energy that can be safely and reliably absorbed is between 0 and 15 kW. In this range the power meter is read directly in kilowatts. Other ranges can be preset on the standby control module requiring different conversion factors for the power output meter.

The control module regulates the flow of water through the calorimeter and provides the necessary electronic circuitry to convert the change in water temperature to power absorbed by the calorimeter. It also has external recorder jacks so that this same signal can be sent to remote recording devices. In addition, a flow switch will turn on a warning light if the flow falls below four liters per minute, which would indicate that the flow rate is too low to absorb laser energy above five kilowatts without damaging the copper cone.

Other Components

In addition to the major components of the pressure chamber, several auxiliary evices have been added to the chamber. One of these is a pressure transducer, intended to continually monitor pressure near the gas inlet. The device selected is capable of high accuracy at elevated temperatures, up to 500C. The transducer serves two functions, one of which is to prevent accidental overpressurization of the chamber. In addition, should a sudden pressure drop occur, it can be assumed that a large leak has developed in the chamber, presumably due to a cracked window. For this reason, the transducer selected (Setra Model 205) has a rapid response time (less than 10 msec).

A second addition is a pressure rupture disk, designed to rupture at 99 psig (at 250F), which will absolutely prevent overpressurization. Like the pressure transducer, it is attached to the chamber using a pressure nipple. In addition to these two nipples, three others have been installed in the chamber as spares, two upstream and one downstream. These can conceivably be used to inject seed particles or to insert a pitot-static tube to measure flow velocity.

Another item is a solenoid-activated air cylinder, shown removed from the chamber in Figure 10. As mentioned earlier, a metal target will be placed at

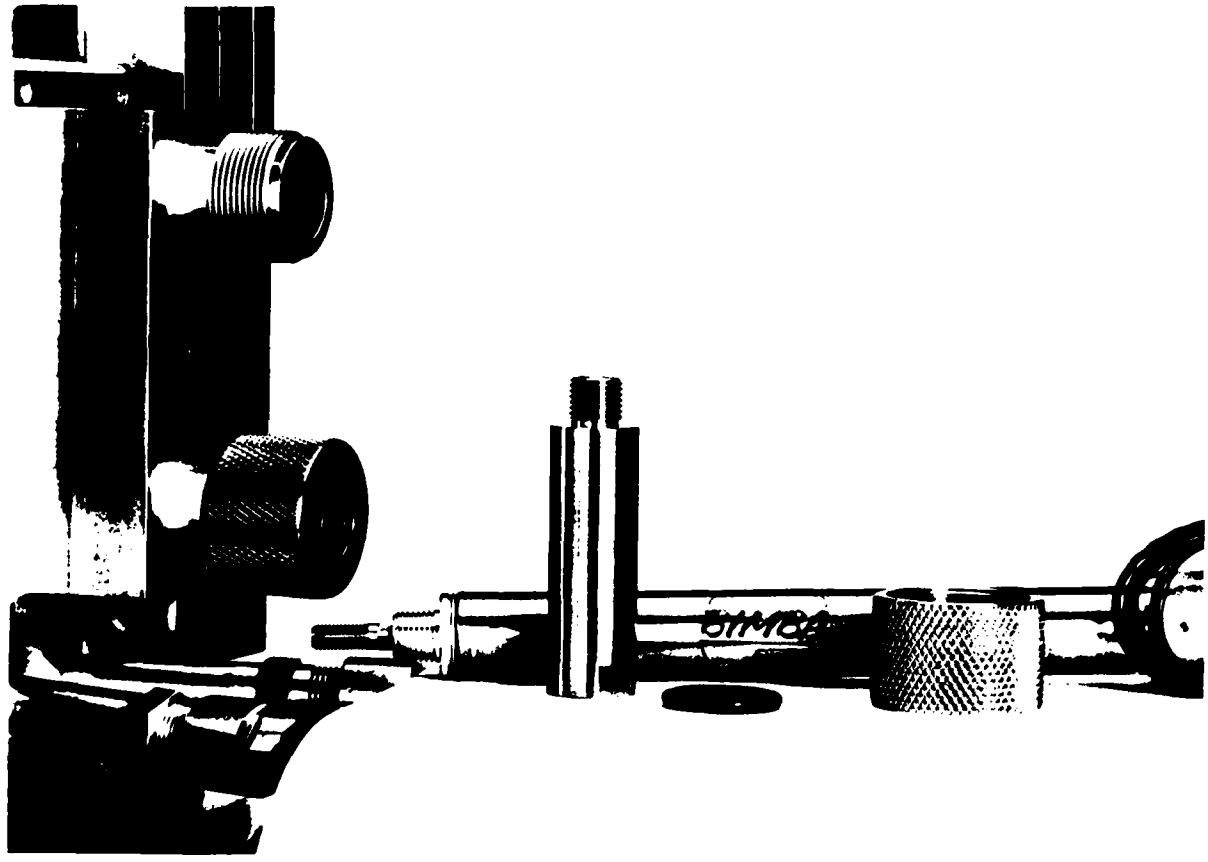

Figure 10 Target Air Cylinder with Seal Assembly

the focus point when the laser is first turned on, then withdrawn once a plasma has been ignited. To do this, the metal target will be attached to a piston arm which is moved in and out of the focus point by the air cylinder. When the solenoid is energized, it opens a valve, allowing high-pressure nitrogen to enter the cylinder. This then forces a piston down to the bottom of the cylinder. The target arm is attached to this moving piston. The cylinder itself is located outside the chamber, but is sealed so that the gas in the chamber will not leak. A recess has been built into the cylinder flange to allow complete retraction of the target, and two seals are included in the flange to allow insertion of the target at two different axial locations. The advantage to this system is that the entire process can be controlled remotely.

Thermocouple Carriage

Another addition is a remotely controlled thermocouple assembly. As was mentioned earlier, we need a means of measuring bulk gas temperatures throughout the flowfield downstream of the plasma. Not only must the system be capable of measuring temperatures at various locations in a two-dimensional plane, but must also move up and down the chamber to sample temperatures throughout the flow.

The design we are using is shown schematically in Figure 11 and consists of several parts. First, a movable round carriage on which the thermocouples are attached is mounted on twin rails in the chamber. The carriage is suspended on a chain that is driven by a programmable stepper motor. The thermocouple wires are routed outside the chamber through an axial slot, and the slack is stored in a pressure-sealed outer box.

The thermocouple carriage is perhaps the most complicated item, and is shown in more detail in Figure 12. The carriage itself is a 0.1875 inch thick

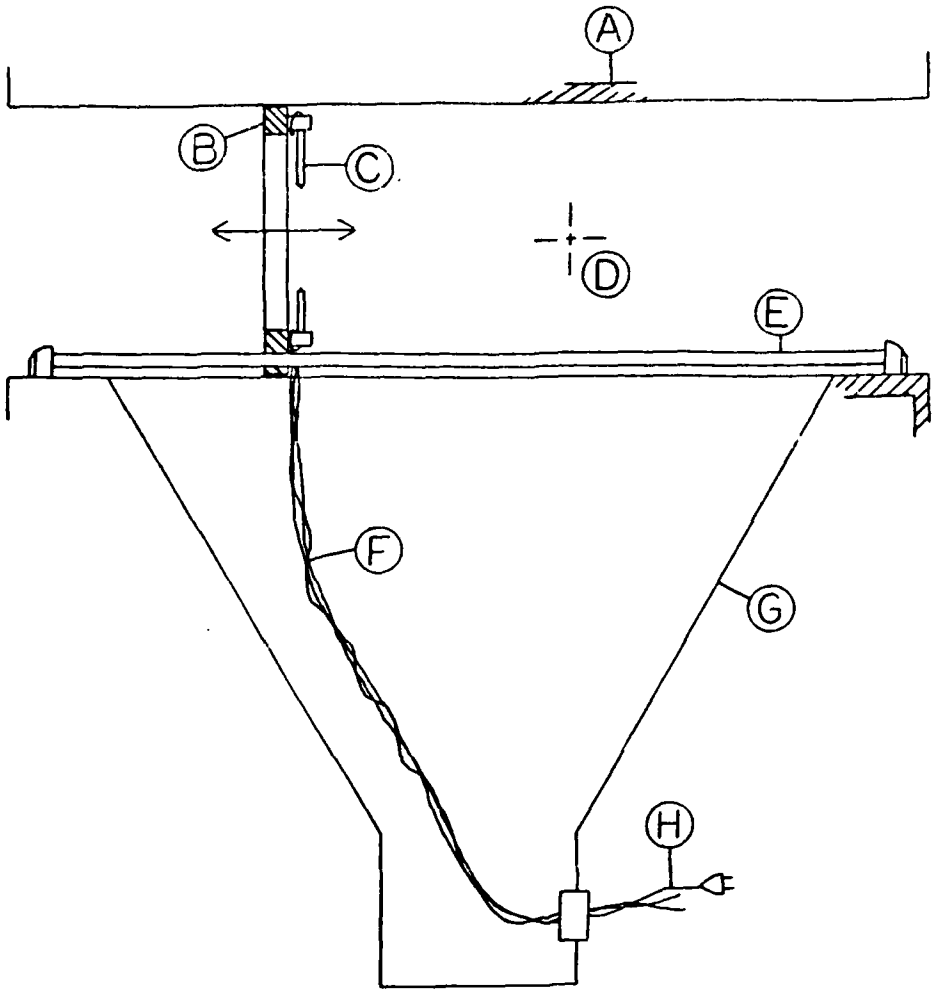

(A) Chamber Wall
(B) Thermocouple Carriage
(C) Thermocouples (7)
(D) Laser Focus Point
(E) Rail Bearing Surfaces (2)
(F) Thermocouple Wires
(G) Thermocouple Wire Retract Box
(H) Connections to Amplifiers

Figure 11 Thermocouple Carriage Operation

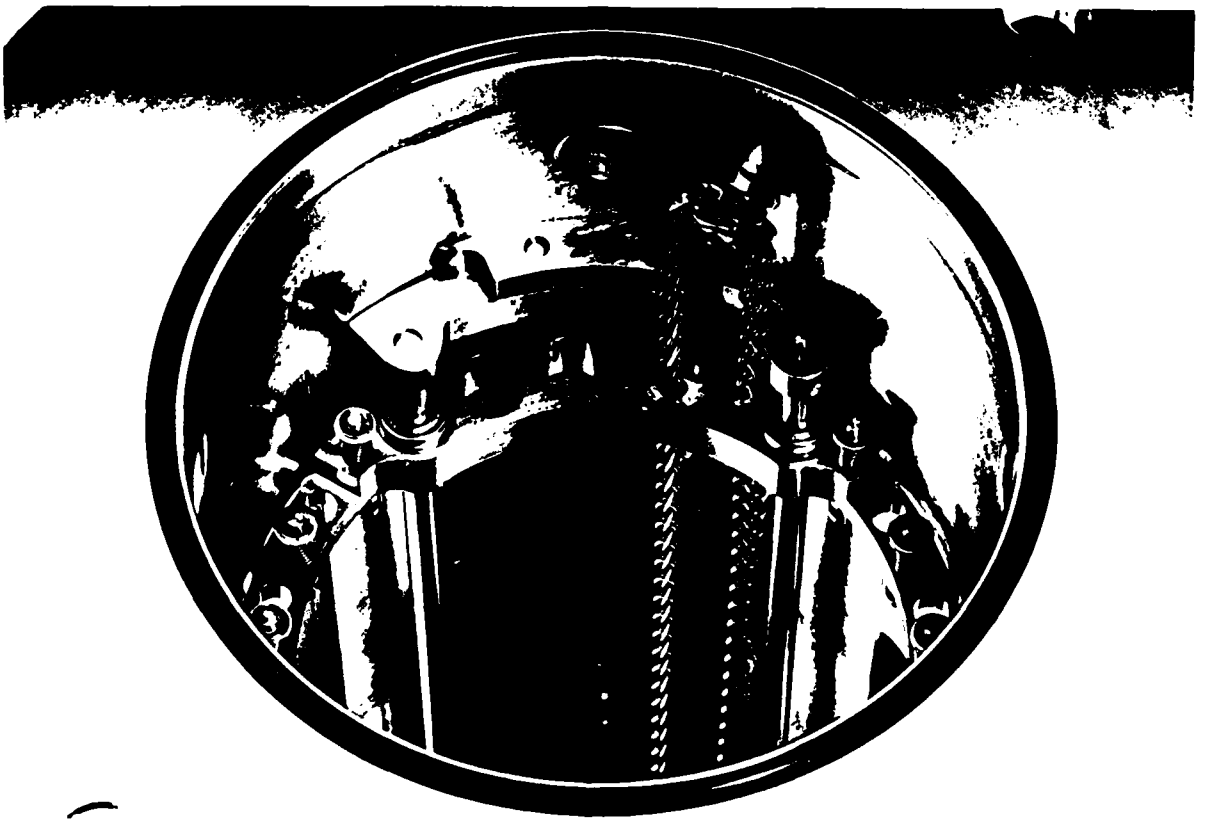

Figure 12 Thermocouple Carriage on Rail Bearings Inside Chamber

cutout of stainless steel through which the two rails run. The rails pass through two precision stainless steel linear bearings that are mounted in the carriage. The rails are precision case-hardened cylindrical rods bearing surfaces that run from the rear of the chamber to three inches upstream of the focus point. Mounted on the carriage are eight pivotable thermocouples of various lengths, each enclosed in hard ceramic insulators (not shown). The thermocouples may be positioned on any of fourteen different pivot locations on the carriage. This combination of thermocouples can measure various sets of points in a two-dimensional plane.

In preliminary tests, it will be necessary to check for radial symmetry in the flow, which requires an ability to measure temperatures at various locations at the same radial distance. In Figure 13, the three sets of circled numbers correspond to some of the sets of symmetrical data points that can be obtained using this configuration of pivotable thermocouples. In later tests, it will be preferable to take a more thorough survey at different radial points by crowding the thermocouples into a single sector. One possible grouping is shown in Figure 13, indicated by crosses.

The construction of the thermocouple pivot mounts is shown more clearly in Figure 14. The thermocouples themselves (not shown) are of the tungsten/tungsten-rediun type, capable of reading temperatures up to 3200K. The thermocouples are first inserted into stiff double-hole ceramic insulators, with the bead left exposed. The naked wires leads are each then wrapped in flexible ceramic insulation.

The ceramic insulator is held in place in a hole drilled through the pivot. The pivot consists of a spring-loaded bolt that runs through the carriage, held in tension by a spring-loaded snap ring. To adjust the position

will be using hydrogen under pressure, the catastrophic failure of a window must not allow the escape of detonable quantities of the gas. Also, some safe method of disposing of the heated exhaust hydrogen is needed, as is a reliable method of detecting leaks.

Several approaches to the problem have been considered. One possibility is to surround the chamber with a fully enclosed hood filled with nitrogen. As seen in Figure 18, this system uses a stainless steel outer box with a see-through front panel, as well as an additional laser inlet window. The nitrogen is slightly pressurized (to prevent air from entering through leaks) and a steady flow of nitrogen is maintained to remove any hydrogen that may leak. The nitrogen can either be exhausted through its own exhaust pipe, or can be combined with the hydrogen exhaust. This entire system virtually eliminates any possibility of a hydrogen fire or explosion. Even the catastrophic failure of a chamber window will not result in direct contact between the hydrogen and air until after the flow has left the building. The only problem with the system is that no reliable leak detectors are available that operate in the presence of pure nitrogen, so there is no way of knowing if hydrogen is leaking into the outer chamber.

Additional safety is possible by locating the chamber closer to one of the windows of the laboratory. This also makes the exhaust problem easier, but forces us to place an additional mirror in the laser beam to redirect it 90 degrees to the window.

If additional safety is needed in the exhaust system, the current two inch (5.08 cm) exhaust pipe can be replaced with one that is used solely for hydrogen, and that extends well above the roof of the building. In either case, nitrogen is added to the flow (in a 90% nitrogen 10% hydrogen ratio) to prevent

what is being recorded. The system accepts up to 10 input channels at a maximum rate of 14 data points per second.

Before being sent to the datalogger, each of the channels is first routed through a control console, from which all experimental systems may be watched by the operator. This console is equipped with two rotary selector dials and several LED displays which allow the operator to continuously monitor chamber pressure, calorimeter output, and any two thermocouples in real time. Should any system begin to exceed its design limits, the laser can be turned off immediately by the laser operator. The console is also equipped with controls for the target air cylinder and for the two stepper motors. The final item on the cart is the OMA diagnostic system and its associated microcomputer display. OMA data will be stored internally, and analyzed using EG&G software. If space permits, the control systems for the tunable dye laser (for LIF) will also be housed in the mobile cart. The IR thermography system has its own mobile stand, and will be placed adjacent to the cart in the control room. The controller for the calorimeter, and the fiber optics and controller for the OMA scanner will both be mounted to the test stand in the laser room itself. All electrical connections between the stand and the mobile cart are routed through the control room wall.

The use of hydrogen presents some very significant new problems. Its low viscosity and high buoyancy (density 1/4 that of air) enable it to escape easily from small leaks in seals and fittings, and to rapidly expand to explosive concentrations in a closed room. Hydrogen also burns readily in air with an invisible flame.

Clearly, working safely with hydrogen means leaks must be avoided and quickly detected so that detonable mixtures are never approached. And, since we

the mass flow valves and runs to the chamber. At the chamber, a "T" is used to connect with the two one-half inch (ID) pipes of the inlet section. The four one half inch chamber exhaust pipes are connected to four flexible, high pressure hoses, which come together in a four way connector. Downstream of this is a valve which fixes the downstream exit area. A larger flexible high pressure hose attaches to this valve using a quick disconnect and will route the gas to a permanent exhaust stack which vents the gas to the outside. Most of the gas line connections are quick disconnect to permit test stand mobility.

The procedure for setting the flow conditions in the chamber consists of three steps. First, the tank regulator is set to provide a specified upstream stagnation pressure. Second, the valve on the rotometer is adjusted to give the desired mass flow rate. The final step entails adjustment of the valve downstream of the chamber to give a chamber pressure close to the one desired. Since this final step will also change the mass flow rate, the two valves must be fine tuned to give the desired combination of mass flow and chamber pressure.

Various flow rates under different pressures will be investigated for each gas used. The mass flow rate depends on the laser power used and the desired bulk exit temperatures, as well as on absorption efficiency and the type of gas used. For example, mass flow rates of 0.5 to 5.0 grams per second will be used with argon, while 0.05 to 0.20 grams per second will be used with hydrogen.

Away from the test stand on its own mobile cart, will be the control and data storage equipment. During the experiments, the cart will be moved into the control room where it will aid in controlling data acquisition and in monitoring safety systems. The main controller is a Fluke datalogger system. This accepts input from the thermocouples, pressure transducer, and calorimeter, digitizes the data, and stores it on tape. A video display is also available to monitor

laser. Before each experiment, it will be necessary to move the station to its positioning holes, then to use the HeNe laser to check that the small mirror receives the beam properly. The laser can also be used to check for alignment in the other mirrors, and to see if the beam is being focused on the metal target within the chamber.

One important problem that must be carefully avoided can occur when a window reflects some of the laser energy being passed through it. For NaCl, roughly 4% of the incident energy will be reflected back into the focusing optics, and care must be taken to avoid damage to the optics or anything else that gets in the way. It is currently believed that nearly all of the reflected laser energy will be recollected by the large mirror and refocused onto the smaller mirror. However, due to the annular nature of the beam, and the fact that the beam will be highly defocused at this point, it is thought that most of the energy will strike the framework around the edges of the small mirror. Detailed ray-tracing work is now underway to confirm this conclusion. Of course, some material must be placed in the areas where reflected laser energy strikes to prevent damage to equipment, but the amount of reflected energy is expected to be small, so simple ceramic materials should be adequate.

The gas handling system to be used with the chamber is designed to allow the use of various gases, to produce steady flow in the chamber at pressures up to 150 psi, and to allow independent variation of the mass flow rate and chamber pressure. The gas is supplied by high pressure tanks located outside of the lab through permanent high pressure lines on site, which terminate at a bank of calibrated mass flow meters (rotometer type). A regulator on the tank fixes the stagnation pressure, and a valve on the downstream side of the rotometers sets the mass flow rate. A flexible, high pressure, gas hose is attached to one of

The mount holding the first flat mirror intercepts the annular laser beam 50.2 inches off the floor and reflects it straight down. This mount is bolted directly to the test stand and permits only gross adjustment about two pivot points. The second flat mirror is positioned directly below this one and can be translated in X and Y space along a dovetailed rail as well as rotated about lines paralleling these two axes. Scales on the rails specify the translation coordinates and two micrometer heads specify the orientation of the mirror in the gimbal mount. Positioned above this mirror is the 4.5 inch convex mirror. It too is held by a gimbal mount permitting adjustments in two directions, but is allowed to translate only horizontally. Two micrometer heads and a scale on the translation rail specify its location and orientation. From here, the beam is reflected down into the 20.0 inch concave mirror. This 250 pound mirror is held in place by a large yoke mount which permits the mirror to pivot about a point at the center of the mirror face. A turnbuckle is used to specify the tilt angle of this mirror.

To facilitate alignment of the mirror system, a model was devised which likened the mirrors and reflected portions of the laser beam to flexible links in a mechanical device. The allowed movements of the four component mirrors in the system are described by three coupled equations, which relate mirror position in X and Y space relative to a datum point (fixed at the center of the main 20 inch mirror) and to mirror tilt. By specifying the focal length of the beam entering the chamber and the tilt of the 20.0 inch concave mirror, the positions and orientations of the remaining mirrors become fixed. The optical alignment model is discussed in more detail in the Appendix.

To assist in aligning the optics, the laser is equipped with an internal low power HeNe laser that can be directed through the main optics of the

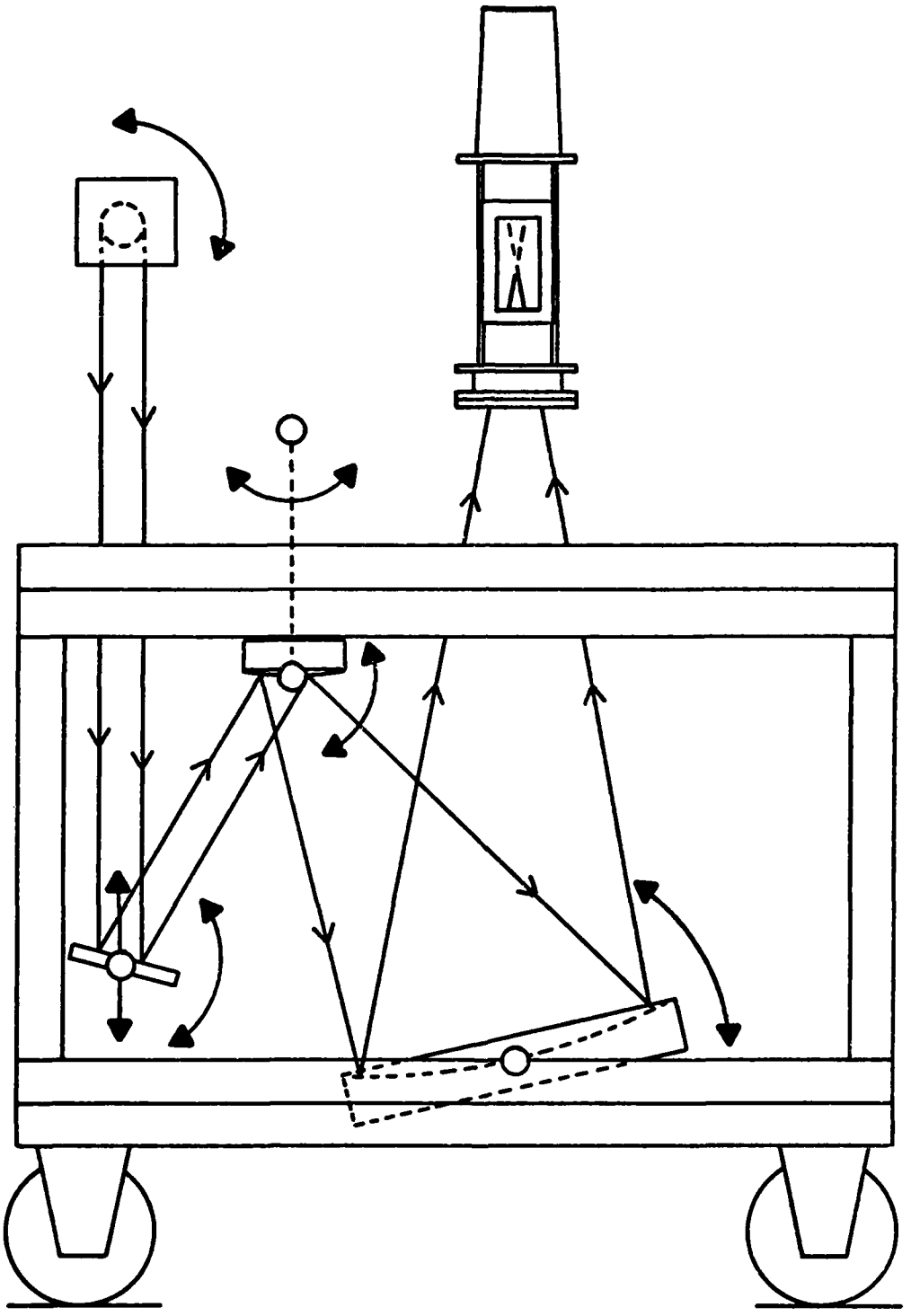

Figure 17 Variable f Number Optical System

plasma from the control room, and for working on the chamber and diagnostic equipment.

As was mentioned earlier, creating plasmas in gases requires a converging laser beam with an F number less than ten. In addition, for various purposes, it is desirable to have the converging beam enter the chamber from below, and for the beam radius at this point to be close to five inches. The existing beam, as it leaves the laser, is a horizontal 2.6 inch (6.6 cm) diameter annular beam 50.2 inches (1.28 m) off the floor. Obviously, some optics must be used to redirect this beam upwards and to force it to converge.

The laser optics we are using are shown schematically in Figure 17. When the laser beam reaches the work station, it is 2.6 inches in diameter and 50.2 inches off the floor. At this point, the beam strikes the first optical component, a 5.0 inch diameter flat, water cooled, copper mirror. This mirror reflects the laser beam straight down into an identical flat mirror, which bounces the beam up into a 4.5 inch convex, water cooled, copper mirror. This mirror spreads the beam and directs it down into a 20.0 inch concave mirror located directly below the chamber. The beam is then focused through the salt window to a specified point in the chamber. A photon drag detector system is used for measuring spot sizes and for final alignments of the optics.

Several objectives had to be considered when designing this optical system. First, the beam had to fill a 4.5 inch diameter area when passing through the salt window, so as to reduce the laser energy flux and prolong the salt window life. Secondly, the focus point of the laser had to be positioned at various points on the chamber center line, but always kept between the viewing windows. Thirdly, the diverging beam downstream of the plasma had to be intercepted by the calorimeter opening of 4.5 inch diameter. These constraints required a system of variable F number between f/2.2 and f/3.6.

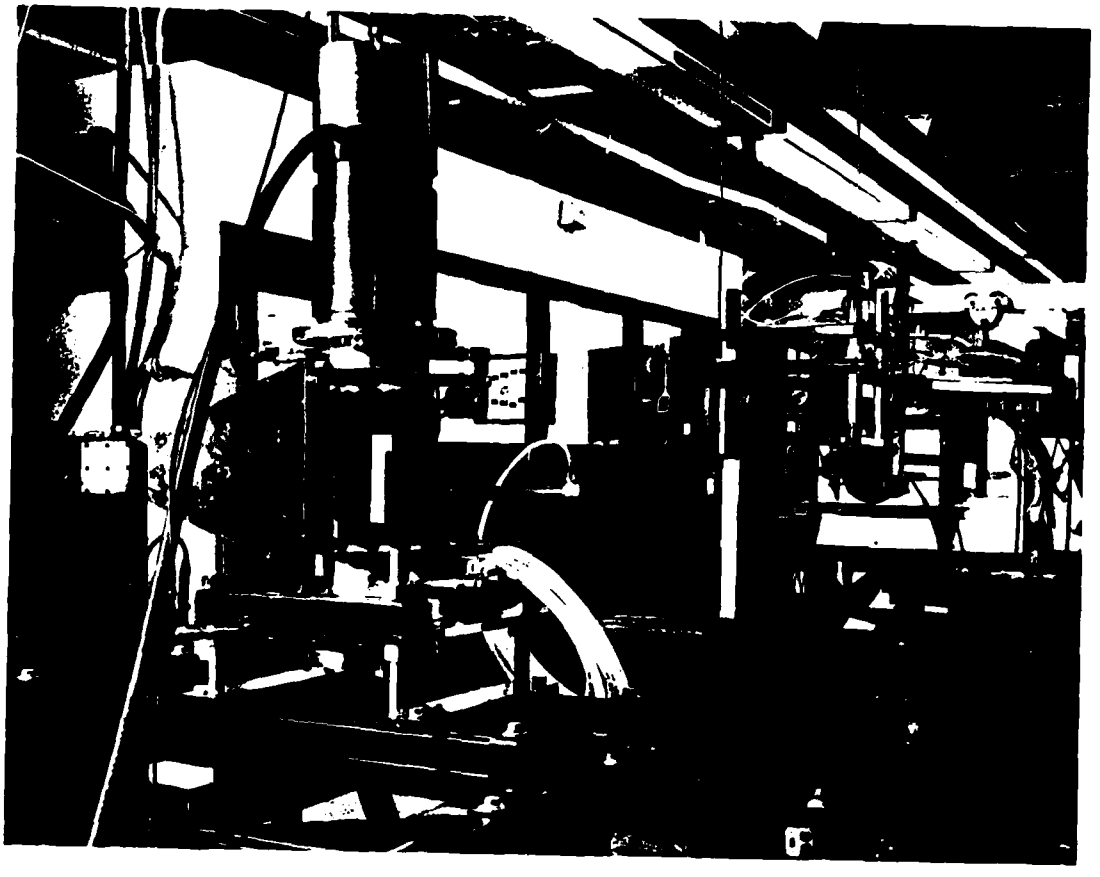

Figure 16 Test Stand in Lab; Laser and Control Room in Background

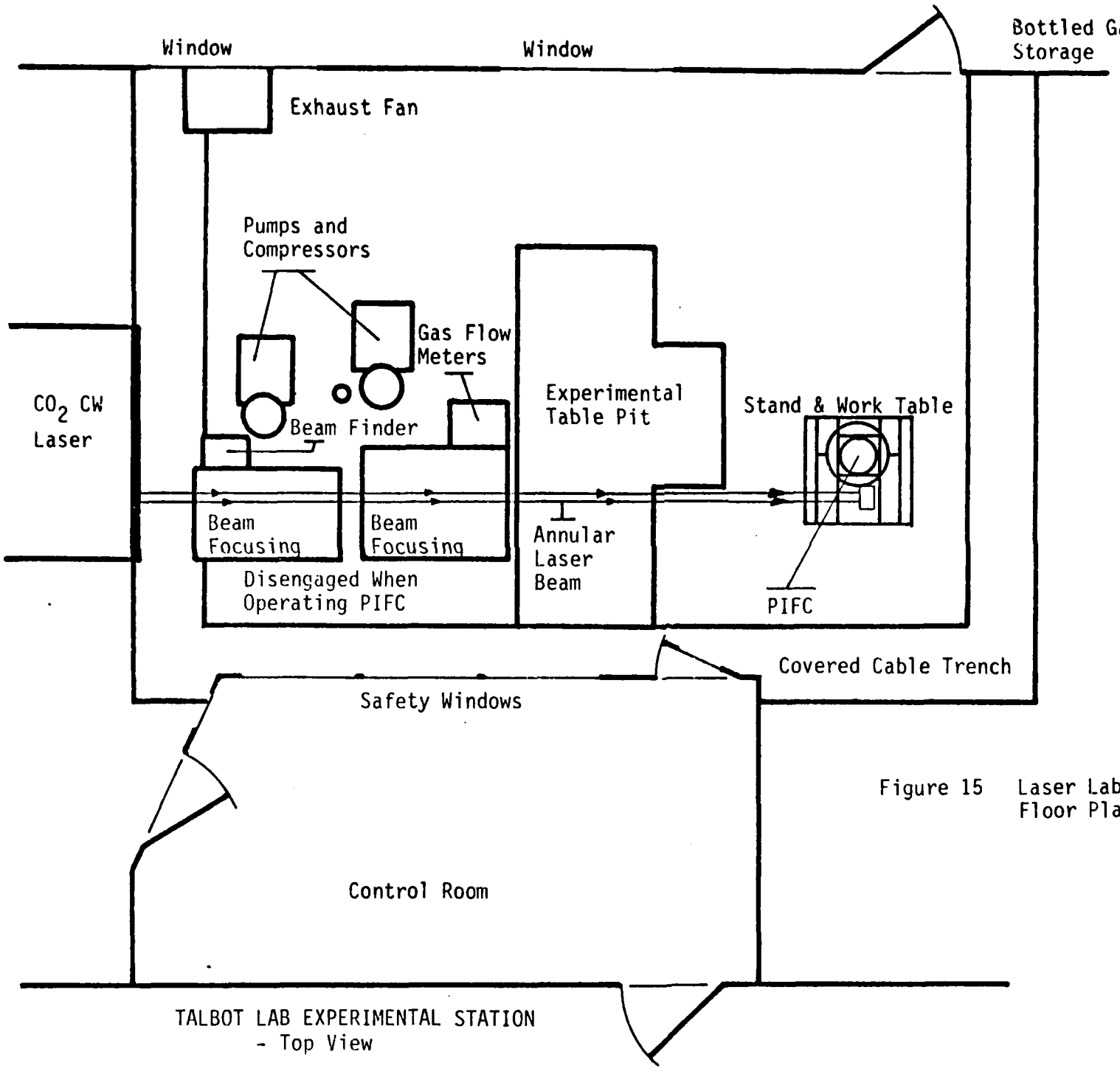

Figure 15 Laser Laboratory Floor Plan

B) Support Equipment

Due to the crowded nature of the laser laboratory, it is necessary for the entire experiment to be mounted on a mobile and self-contained test stand. The stand, which consists of a rigid frame on rubber wheels, holds the laser optics, the chamber, and all diagnostic and support equipment, is capable of relatively precise positioning on the floor, and will hold any safety systems required when hydrogen is used.

The location of the test stand in the lab is shown schematically in Figure 15. This location was selected because it allows us to use the laser beam directly without the need for costly redirections of the beam. Also, placing the chamber here permits direct observations from the control room, and the site is fairly close to both the gas inlets and the exhaust piping.

The frame itself, together with much of the equipment, is shown in Figure 16. The stand is made from bolt-together Unistrut because of its strength and versatility. The laser optics, which convert the parallel beam into a converging beam, occupy the lower half of the frame, the chamber is in the upper half, and the diagnostic instrumentation will be placed on shelving near the chamber viewing windows. Rubber wheels are attached to the base of the frame for easy mobility, but the stand can be precisely positioned using pins that fit into positioning holes in the concrete floor. The pneumatic tires also serve another function: damping out vibrations caused by pumps and compressors used to operate the laser. The stand itself weighs 400 pounds, while the combined weight of stand, chamber and attached equipment is about 900 pounds. The stand base was made wide and the center of gravity set low to prevent accidental toppling. This also leaves the chamber at a convenient height for viewing the

thermocouple is inserted into one of the four exhaust lines to measure bulk exit temperatures. All of these thermocouples must of course attach to an analog recorder of some sort; this will be discussed later.

of the thermocouple, the bolt is turned slightly. The advantage of this arrangement is that both the ceramic insulators and the shielded thermocouples can be quickly replaced and/or adjusted. To do this, it will of course be necessary to remove the calorimeter so that we have access to the inside of the chamber.

From the pivot, each thermocouple wire (each three feet in length) is routed around the circumference of the carriage, utilizing the spring-loaded portion of the pivot bolts as a harness, to the slotted flange in the side of the chamber. Here, all the wires are joined in a bundle and passed through the slot to a box sealed to the chamber. This box holds the wire slack which is needed as the carriage traverses the length of the chamber. The thermocouple wires are routed through holes in the side of the box, then through a pair of rubber gaskets which pinch and seal the wires. Finally, the wires are connected to cold junction references and amplifiers.

To drive the carriage, a programmable stepper motor is used. This motor, like the target air cylinder assembly, is mounted outside the chamber, but the drive shaft passes into the chamber through a set of O-ring seals. The motor turns a one-half inch sprocket which drives a chain that suspends the carriage. The motor uses software interfacing which allows a variety of programmed motions, but is also designed to be overridden manually if the operator detects one or more of the thermocouples entering temperature regions above their design limit (3200K).

In conjunction with the thermocouple carriage, two other thermocouples will be used. One is mounted on the wall of the chamber, near the focus point, to monitor wall temperatures. This is very important to ensure that the temperatures of the two viewing windows do not exceed their design limit. Another

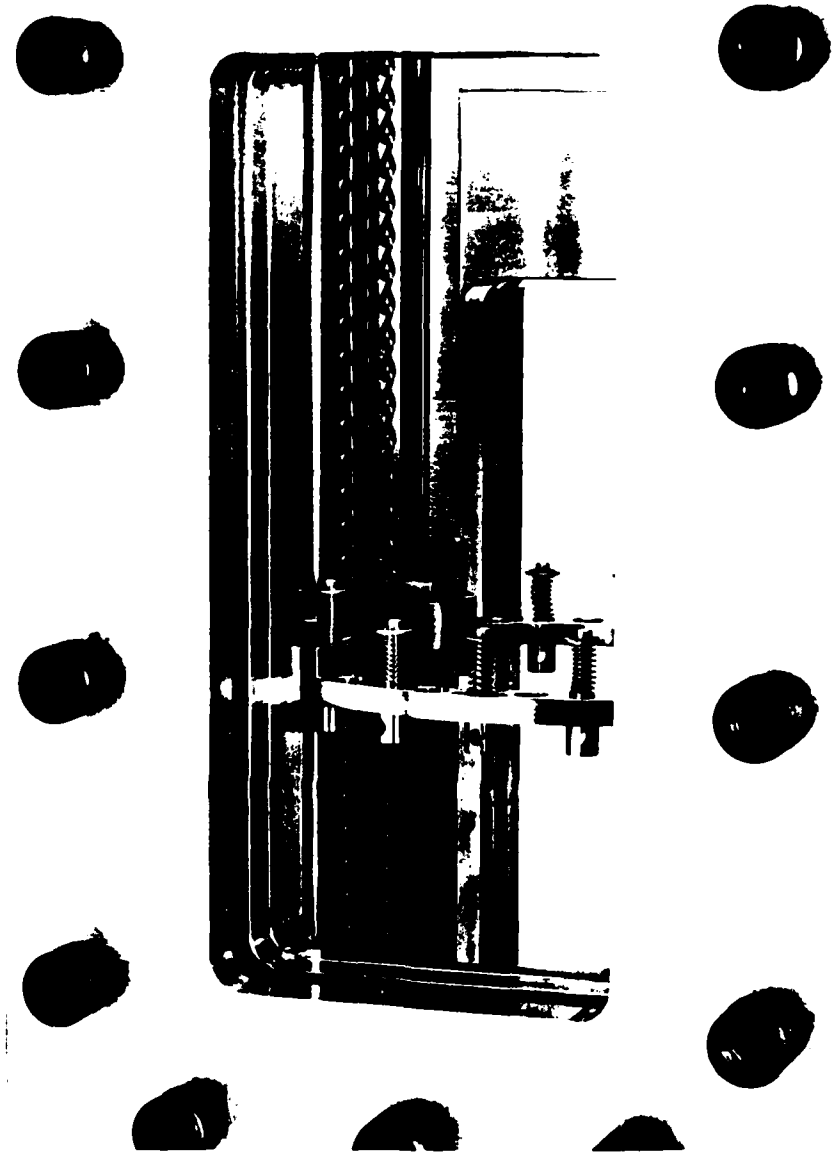

Figure 14 Close-up of Thermocouple Pivot Mounts

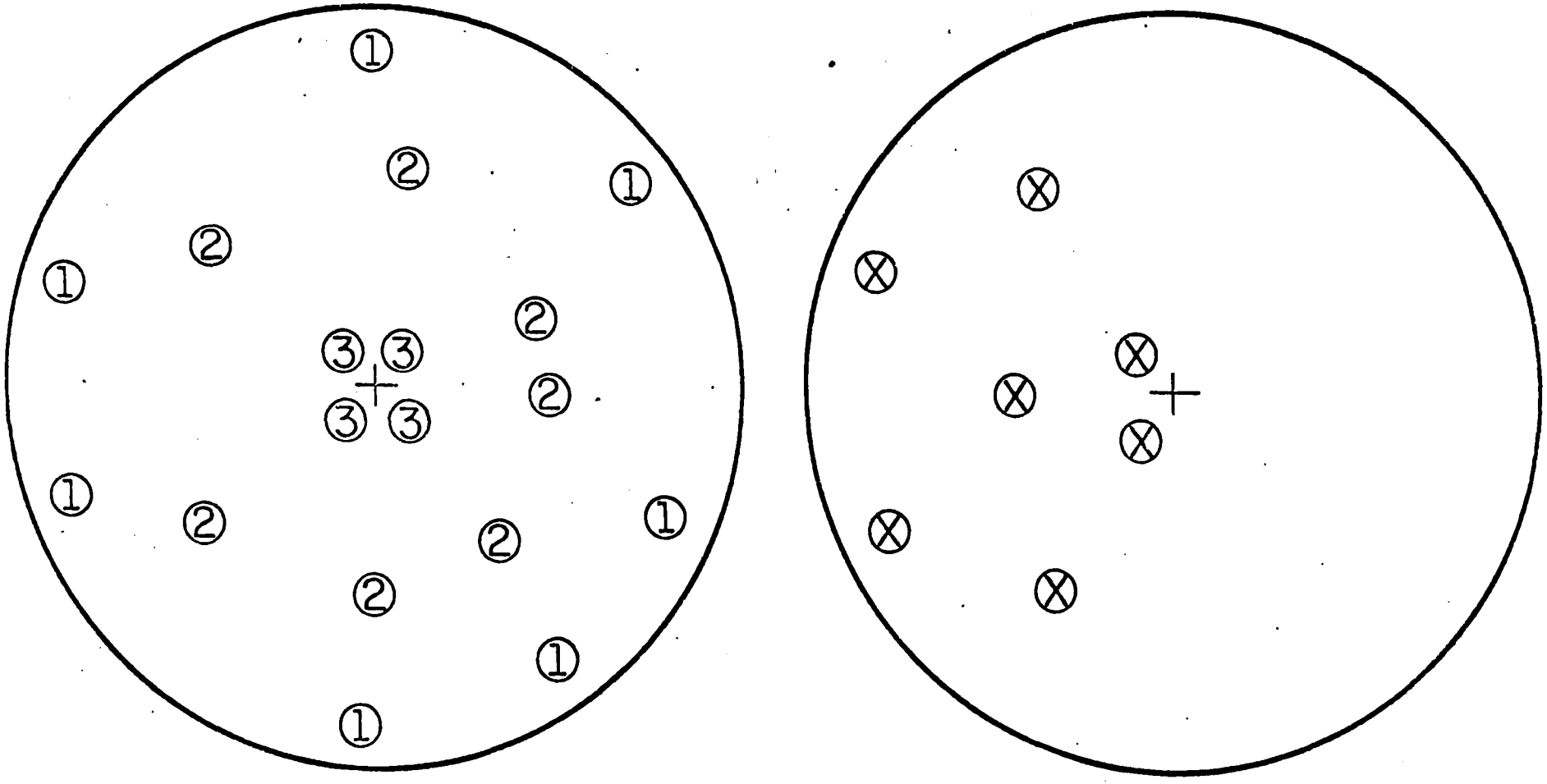

Figure 13 Thermocouple Data Sampling Groups

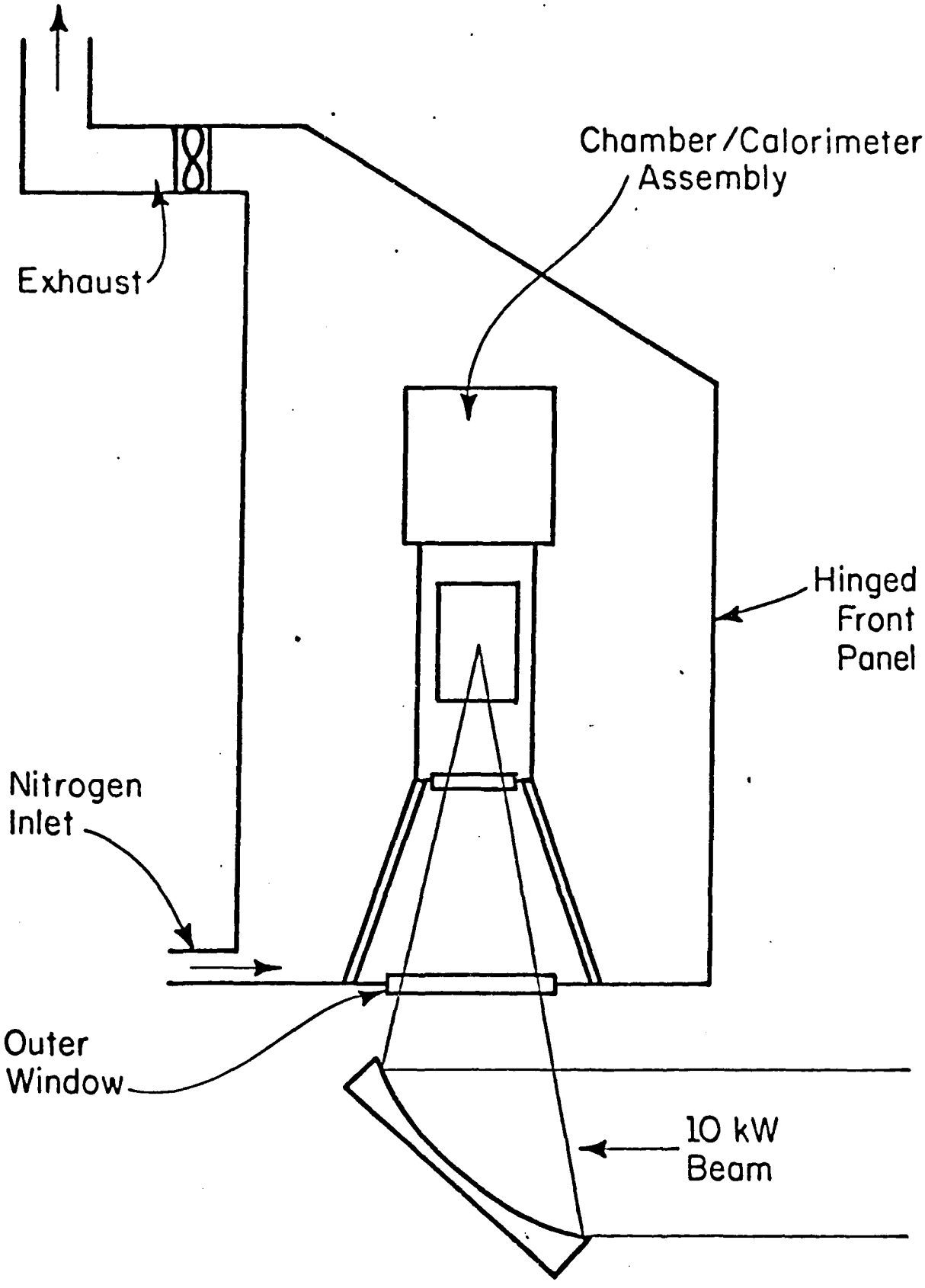

Figure 18 Hydrogen Safety Enclosure

fires or explosions in the pipe. The idea of using a hydrogen combustor on the roof was dropped due to the low mass flow rates of hydrogen being used.

To detect leaks of hydrogen, several devices are available, all of which are relatively accurate and highly reliable. Currently, we plan to mount several detectors above the work station and feed their output into an alarm system. Heat detectors will also be used to detect fires. Every effort will be made to ensure the safety of the researchers while eliminating any possibility of damage to personnel, equipment, or the laser laboratory.

IV) DIAGNOSTIC TECHNIQUES AND EQUIPMENT

A. High Temperature Diagnostics-Spectroscopy

The high temperatures encountered in the core of a laboratory plasma (approaching 20,000 K) prohibit the use of conventional temperature measurement techniques. The two most widely used diagnostic techniques are laser interferometry and spectroscopy. But since the vibration-prone environment of our laser facility renders laser interferometry impractical, spectroscopic analysis will be used.

A full understanding of the dual-flow process requires not only a knowledge of the bulk gas (or ion) temperature, but also the temperature and number density (N_e) distributions of the electrons. To accomplish this, we will be making spectroscopic measurements of relative line intensity ratios and line broadening of spectral lines. We will also utilize absolute line and absolute continuum methods as independent data checks. Most of the spectroscopic techniques have reported errors of 10-20 percent.

The relative intensity of spectral lines is a fairly simple measurement technique. By assuming that the various energy level populations obey Boltzmann statistics, the line intensity can be formulated as a function of number density and electron temperature. Once the intensity ratio of two lines of the same element has been measured, the number density cancels, leaving the ratio as a function solely of temperature. Thus only one type of measurement must be performed to analyze electron temperature. Number density can then either be calculated from the Saha equations, or measured directly. Calculating transition probabilities and statistical weights of the various lines is a source of error which typically requires the use of well documented particles such a hydrogen,

helium, nitrogen, and argon. Number density may also be independently analyzed by measuring broadening of spectral lines.

Initially, we intend to use argon as the plasma gas. Argon has well documented physical properties [8, 9, 10] and has been the focal point of several investigations [11, 12, 13, 14]. Key, et al. [11] have used relative line intensities of the ion/atom lines of argon (458.99 nm/457.9 nm) to measure temperatures from 8000 K to 15,000 K. Figure 19 is an example of data from [11]. Most of the scatter in the data is attributable to arc geometry, electron density, and the Abel inversion. Kobayashi and Suga [12] have used the ion/atom lines (430.01 nm/434.81 nm) to measure a similar temperature range. Tsao and Pavelic [13] have used the 415.86 nm and 425.94 nm atomic lines of argon to measure temperatures from 3000 K to 8000 K. Therefore, by using two pairs of lines, we may quantify nearly the entire temperature range of interest. This should be useful in assessing the merit of the various medium temperature range diagnostics to be subsequently discussed.

To determine electron number density in argon, it is best to use absolute line intensity [8] or absolute continuum intensity [8, 10, 16] methods. Both methods require a calibration source such as a tungsten filament lamp. As noted in [16], however, the number density can be reduced to a relatively simple function of continuum intensity and electron temperature. Since we will have already measured electron temperature via relative line techniques, it should be possible to calculate density by measuring a band of continuum radiation near one of these lines.

Since we will eventually be analyzing hydrogen plasmas, it will be beneficial to use hydrogen as a seedant in our studies of argon plasmas. Schumaker and Wiese [14] have used hydrogen as a seed in argon and nitrogen, using

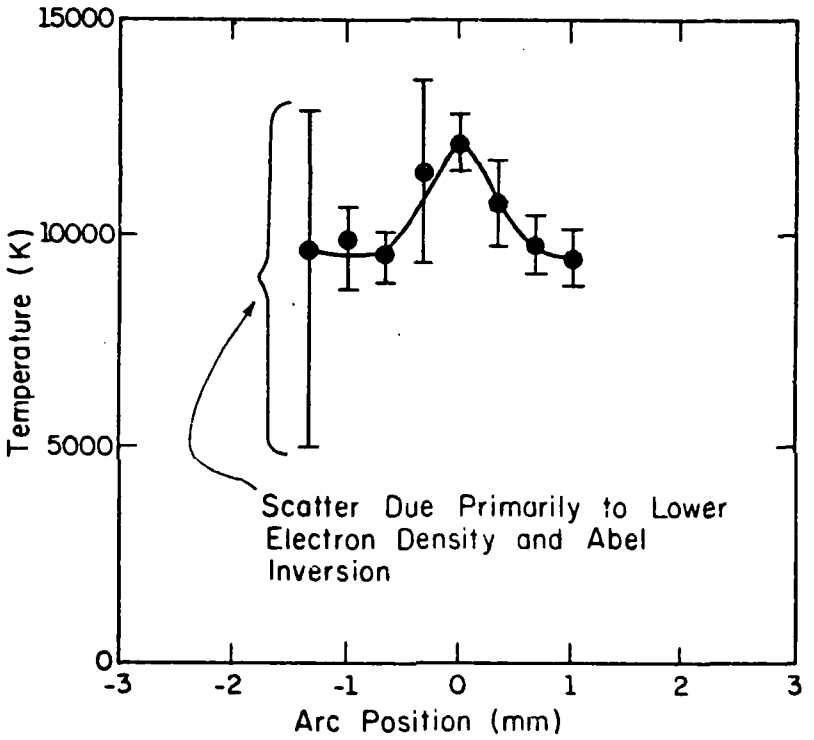

Figure 19 Radial Temperature Distribution in Argon Plasma (From [11])

hydrogen line broadening theory to determine N_e. They also report the absolute intensity measurement of the argon ion line (480.6 nm) using a tungsten lamp calibration source. We will investigate all of these techniques as an independent data check.

Eventually, we will move on to plasmas in hydrogen, where we will use the ratio of the Balmer series H_β line to continuum radiation to measure electron temperature. Figure 20 is a typical Stark-split H_β profile. By measuring approximately 10 nm of continuum radiation near the H_β profile the continuum radiation below the H_β profile can be extrapolated. The line wings of the H_β line will first be extrapolated (dashed lines). We will then numerically integrate the profile and subtract the underlying continuum radiation, resulting in the line intensity. The ratio of the line intensity to continuum intensity yields temperature. For our range of interest, errors should be < 10% [8], as long as the H^- continuum is avoided (T < 10,000 - 12,000 K). This technique is rather forgiving as deviation from LTE should not affect the Balmer lines for $N_e > 10^{14}$ cm^{-3} [8].

Number density can be calculated from the Stark broadening of the H_β line [8, 10, 14]. For our expected range of N_e, (10^{15} - 10^{17} cm^{-3}), the predominant broadening mechanism should be a linear Stark effect [8, 15]. Therefore, one may use the tabulated values of [8, 10, 14, 15] to calculate N_e directly from measurements of the Stark broadened half-width.

Another technique which may be possible is to seed the hydrogen with argon. The argon line pairs mentioned previously could be used to measure the entire temperature range (3000 - 17,000 K). More work is needed to calculate seedant quantities required to measure the argon lines and to see if the argon lines will be resolvable in the presence of hydrogen.

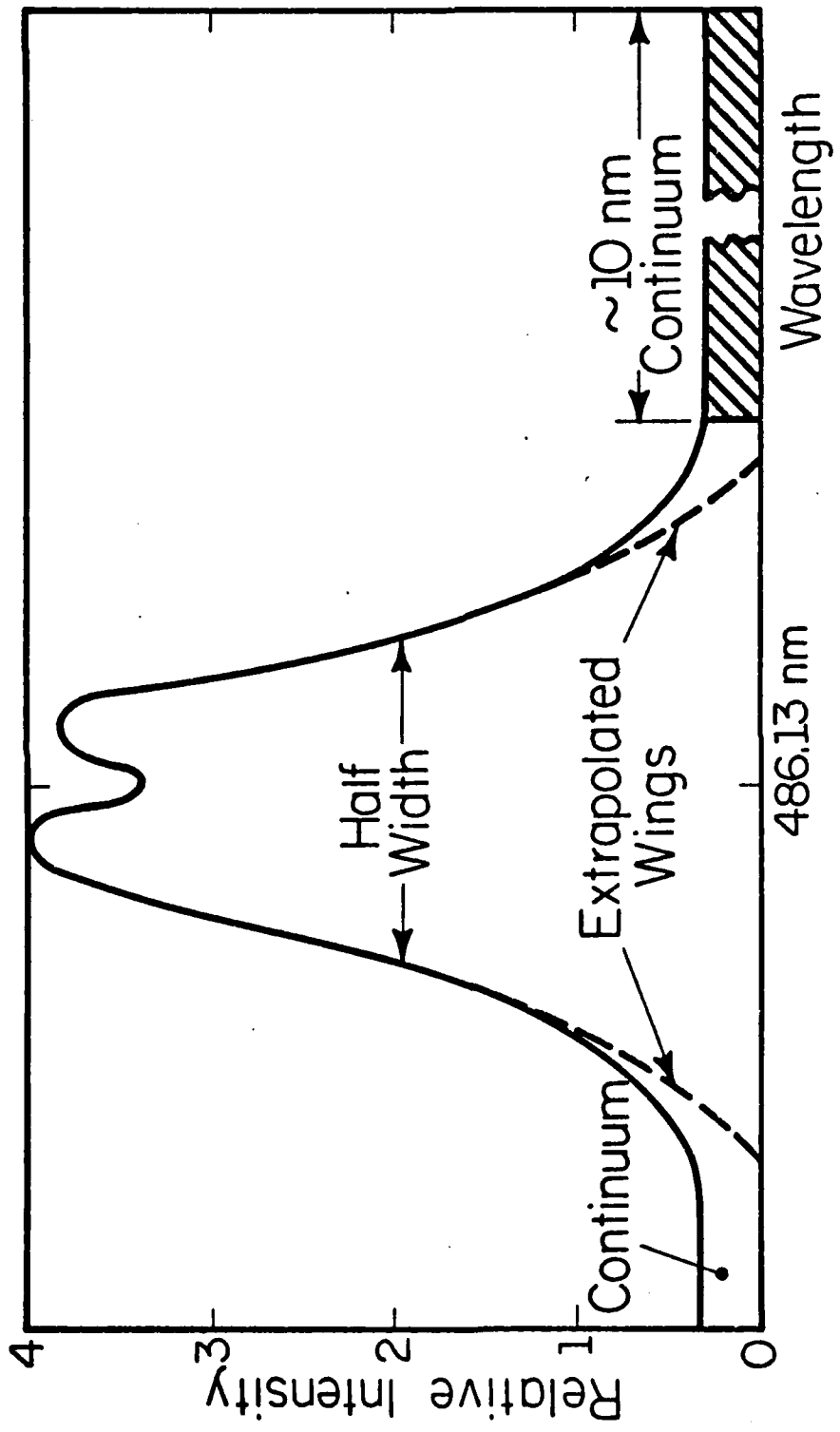

Figure 20 Stark-Split Profile of Balmer Series H_β

At some point, it may be desirable to use nitrogen as the plasma gas. Nitrogen plasmas have been analyzed by several researchers [14, 16]. Again, we will use a two line relative intensity technique to determine temperature from the ion/atom pair, 399.5 nm/413.76 nm. The multiple species present (N, N^+, and N_2^+) in our temperature range may make the calculation of partition functions difficult and the number of Saha equation unwieldy. Myronuk and Soo [16] measured the absolute intensity of the nitrogen continuum at 495.5 nm using a tungsten lamp to calibrate N_e. For this case, temperature can be reduced to a relatively simple algebraic function of measured intensity and N_e.

Shumaker and Wiese [14] have used hydrogen as a seed in nitrogen plasmas, again using line broadening theory to calculate N_e. Another candidate follows the work of Keefer, et al. [17] on air plasmas. The emission coefficient of the N_I 493.5 nm line should pass through a maximum in our temperature range of interest. One may then match the peak measured radial emittance to the calculated emission coefficient peak. A Fowler-Milne spline-fit is used to reduce the remainder of the temperature field.

To perform the spectroscopic measurements we will be using an optical multichannel analyzer (OMA) manufactured by EG & G. The OMA consists of sensing, storage, and processing equipment used to measure spectral line intensity as a function of time and wavelength. The OMA system includes a monochromator, detector, detector controller, and processing unit. Each line scan of the plasma is sent to the monochromator via an optical fiber. The fiber is moved across the plasma on a rail driven by a programmable stepper motor. The monochromator spectrally disperses this narrow band of emitted plasma radiation across the face of a silicon intensified target (SIT) detector. The SIT is a vidicon detector (2 dimensional array) which will allow scanning of a complete

cross-sectional area of the plasma. The SIT detector is also a preamplification stage for input to the detector controller, which is a 16-bit computer peripheral supporting scanning and digitization of SIT information. The console is a micro-computer based processor which controls the system operating parameters and manipulates data. The processor has the capability of 2D plotting of time resolved events; background subtraction; curve smoothing, fitting and integration; and can be user programmed for other processing such as Abel inversion. The console has a CRT for on site data display and a flexible disc for storage.

The plasma will be initiated and sustained in a vertical chamber. This will provide a radially symmetric plasma which allows the inversion of measured line-of-sight intensities to radial emittances using the Abel inversion [18]. Following the work of most plasma investigators [11, 16, 17] we will intially assume LTE (local thermodynamic equilibrium - Boltzmann statistics) and that the plasma is optically thin. After we have performed the measurements we will check the assumptions using the self-consistency checks outlined in Griem [8].

B. Low Temperature Diagnostics/Infrared Thermography

Measurements of the plasma core are useful for studying absorption behavior and other high-temperature phenomena, but in order to fully understand the dual-flow process, temperature surveys need to be made of the cooler downstream mixing zone. As was discussed earlier, at very low temperatures (<3200 K) thermocouples will be used. At slightly higher temperatures (up to 4000 K), we will attempt infrared thermography of the gas.

The University of Illinois (Department of Mechanical and Industrial Engineering) owns an Inframetrics Model 525 Infrared Scanner system. We intend

to use infrared thermography for downstream flow visualization in the sub-4000 K temperature range. Unfortunately, the Model 525 system is calibrated for sub-1000 K temperatures. To increase the range of the system, filters have been added to calibrate the system to 2000 K, although we are currently limited by a 1200°C temperature source.

The Model 525 detector is a Hg:Cd:Te semiconductor which counts photons in the 8-12 μm range. The detector/electronics package operates in the -80°C to 500°C temperature range. From Maxwell's radiation model, it is seen that at all wavelengths more photons are emitted at higher temperatures. Since the detector senses 8-12 μm photons, a filter which attenuates the number of photons at 8-12 μm will prevent detector saturation at elevated temperatures. Most optical glasses have sharp cutoffs at 1-2 μm and remain fairly linear to 20 μm, transmitting less than 1%. Pyrex glass was chosen for the above reasons and its resistance to flow at elevated temperatures.

A box oven capable of attaining 1200°C has been used for calibration. A boron crucible with a conical opening and a small, deep hole at the vertex was used as a blackbody source. It was found that a 3/8" thick pyrex optical flat would prevent detector saturation at 1200°C. A thermocouple in close proximity to the black body monitored temperature and a data point was measured every 20°C as the blackbody cooled from 1200°C.

The detector/electronics package is fairly linear over the output range which allowed linear extrapolation of the sub-1200°C data out to 2000 K as seen in Figure 21. With additional filtering and higher temperature calibration sources, it appears feasible to extrapolate the response to 4000 K. We are currently seeking results using a 2000°C calibration source. Future work will also evaluate the effects of temperature gradients between the detector and source.

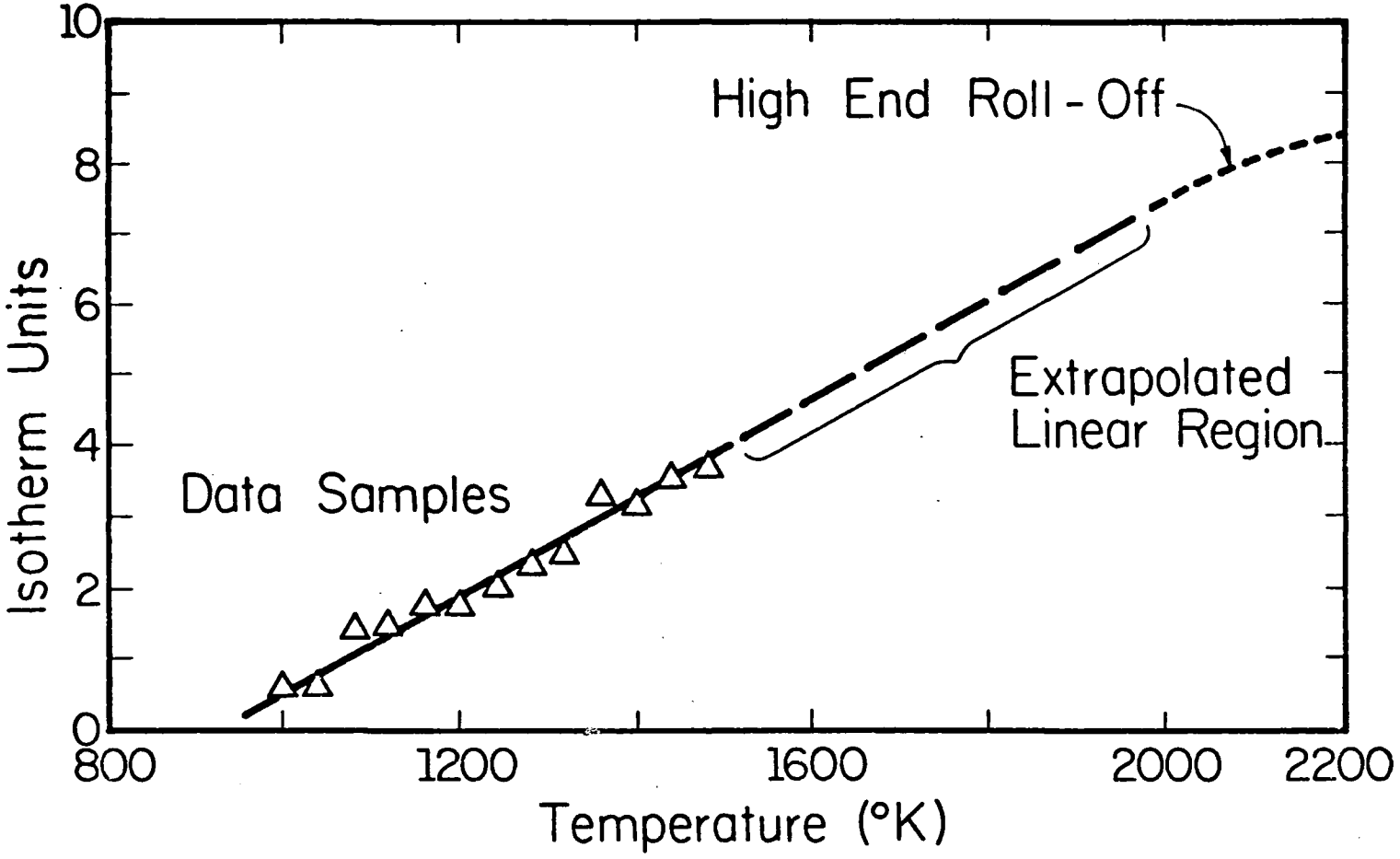

Figure 21 Blackbody Calibration Data - IR Thermography System

In applying the Model 525 system to flow visualization, emissivity data will need to be known for the various gases in order to provide quantitative results. Little or no emissivity data has been found in the literature for the gases we intend to use. Experimental measurements may be a solution. We have attempted to predict emissivities of Al_2O_3 and MgO using our blackbody calibration curves and comparing the data to values in the TPRC reference manuals [19] with only moderate success due to lack of reference data. The various problems associated with measuring the emissivities of gases are yet to be worked out. Nevertheless, it should be kept in mind that this technique is most valuable as a qualitative means of flow visualization, and as an independent means of checking thermocouple data.

C. Medium Temperature Diagnostics - Laser Induced Fluorescence

The preceeding sections have outlined our experimental procedures for measuring high (> 10,000 K) and low (<4,000 K) gas temperatures. In all but one case (argon), there is a need for a separate measurement method for the 4,000-10,000 K temperature range. Little or no experimental work other than interferometry has been performed in the 4,000-10,000 K range. Interferometric techniques, however, were shown not to be applicable to our particular research. This section outlines a proposed temperature measurement technique which should provide considerable information on the flow mixing which occurs in this temperature regime; namely, laser induced fluorescence (LIF).

Basically, LIF is the process in which a particle (typically a seedant) is excited into a higher energy state by a multiple wavelength laser system which has been tuned to the transition of interest. As the particle relaxes via fluorescent decay, the fluorescent photons can be monitored, the resulting intensity being proportional to the number of particles present and their temperature.

Recent advances in laser induced fluorescence (LIF) [20, 21, 22, 23] have demonstrated its usefulness in temperature measurement. Moreover, Hanson [21], among others, has utilized LIF as a quantitative flow visualization technique. Hanson has also made use of planar LIF, permitting the evaluation of an area, rather than a point, on a single shot basis, which increases data acquisition rates. Although the reported LIF techniques were used to study combustion reactions ($T < 4{,}000$ K), there is nothing in the physics of LIF which precludes extension to high temperatures, as long as the seed molecule being studied does not decompose.

The selection of a seed particle may be our most difficult problem. Since we intend to measure temperatures approaching 10,000 K, the particle should have an ionization or dissociation energy of 10 eV or greater. This will reduce the number of species present in the system, minimizing the measurement effort. The particle should also be non-reactive within the system, and have a low absorption cross-section at the 10.6 μm laser wavelength. Finally, since the plasma core temperatures will approach 20,000 K, the seedant should be introduced downstream and homogeneity must be insured.

The equipment necessary to perform LIF measurements includes a tunable laser system, detection and storage equipment, and displays. Most investigators have used an ion laser to pump a dye laser. The dye laser can be tuned to various wavelengths by changing dyes and frequency doubling. The resultant laser beam is then optically transformed to a plane which intersects the plasma plume parallel to the axis of symmetry. The fluorescent radiation emitted by the gas is then monitored using a vidicon-type detector with narrow band filtering. In our experiments, the detection, storage, and processing equipment of the previously described OMA system would be used for LIF measurements. The

planar tunable laser beam is introduced into the pressure chamber by removing the thermocouple wire retract box and replacing it with a transparent window.

In addition to LIF, other temperature measurement techniques merit further evaluation. Babelot, et al. [24] have developed a multi-wavelength optical pyrometry system for temperature measurement up to 10,000 K. Although the system measures a single point, it has a sub-picosecond repetition rate and requires little or no a priori knowledge of quantities or constituents to be measured. Another family of temperature and number density measurements involves laser absorption and refraction [25]. These methods are non-perturbing and relatively simple to implement, using a small HeNe laser. Since we expect number densitites in the range of 10^{15} - 10^{17} cm^{-3}, laser techniques may be viable. Finally, as mentioned previously, we may be able to use argon as a seed gas to measure temperature from 3,000 K and up [11, 12, 13], via relative line intensity spectroscopy. More work is needed to evaluate the effects of the necessary quantities of argon on a given (hydrogen or nitrogen) system. The last two techniques mentioned both make use of the OMA detection system.

V) FUTURE WORK

During the first year of the research program, most major pieces of experimental equipment were designed, built, and installed in the laser laboratory. This includes the pressure chamber, much of the chamber support equipment, the laser optics, and the test stand. The chamber has also recently been pressure tested. In addition, various techniques for measuring gas temperature have been examined, and several have been selected for use. Some of the diagnostic equipment has been purchased, and the data recording and analysis systems are now being readied.

In the near future, we will be completing the final preliminary steps before experiments can begin. The first priority is to complete the mirror mounts for the four mirror optical system, and to align the mirrors. Once this has been completed, and the sodium chloride windows have been successfully tested, initiation experiments in non-flowing argon can begin. In the meantime, the chamber flow system will be tested for steady uniform flow at various mass flow rates and chamber pressures. Following this, the initiation experiments can be extended to flowing argon.

The initiation experiments will focus on the formation of plasmas using retractable metal targets and metal vapor seedants as the source for free electron cascading. Initiation and maintenance intensities will be measured as functions of chamber pressure, mass flow, flow velocity, beam geometry, and seed concentrations. We will also try to find conditions under which plasma instabilities occur.

Following these initial experiments, calorimeter and thermocouple data will be gathered in argon under various pressure and flow conditions. At the same time, the infrared thermography system will be tested and its results will be

compared to thermocouple data. Data analysis for this system will hopefully be improved.

By Fall, 1984, temperature and number density surveys of the plasma core region should begin in argon, using the OMA system. Before this goal is reached, all components of the diagnostic system need to be purchased, the data analysis techniques and associated software must be in place, and the detector assembly must be installed on the test stand. In argon, since spectroscopic analysis may be used down to near the upper temperature limits of the thermocouples, complete surveys of downstream mixing behavior should be possible. We hope to examine ways of improving the efficiency of the mixing process by changing flow patterns and beam geometry.

As we move into the third year of this program, emphasis will shift to experiments in hydrogen. The complete range of experiments that were conducted in argon will be repeated in hydrogen. At the same time, the LIF diagnostic system will be installed and tested. Potential LIF seeds still need to be chosen, and data analysis procedures worked out. Spectroscopic techniques for hydrogen will have already been tested in seeded argon, so plasma core studies should be straightforward.

VI) APPENDIX

As was discussed in Section III, a variable F number optical system will be used to position and focus the laser beam. This flexibility is needed in order to reduce energy fluxes through the NaCl inlet window, to permit vertical focusing of the beam at several locations within the chamber, and to examine the effect of beam geometry on plasma size and stability.

As was shown in Figure 17, four mirrors are used. Two flat mirrors direct the beam to the 4.5 inch convex secondary mirror, which in turn expands the beam onto the 20 inch concave primary mirror. By moving the secondary mirror relative to the primary, the F number of the system can be varied from 2.2 to 3.6.

According to the manufacturer, aberrations in the system can be minimized by fixing the primary mirror (allowing rotation only) and pivoting the secondary mirror about a non-fixed twelve-inch radius arc, the focus of which is also the center of the radius of curvature of the primary mirror. Specifying the exact location and orientation of the secondary mirror is somewhat complicated, so a pseudo-mechanical model of the optical system has been devised.

The geometry of the model is shown schematically in Figure 22. The primary mirror is assumed fixed at location 1, its orientation with respect to the vertical specified by the angle ψ. Since F number and focal length both depend on this orientation angle, ψ is used as the independent variable. L_1 and L_2 are the radii of curvature of the primary and secondary mirrors, respectively. Location 4 is the point about which the secondary mirror is assumed to move. Note that the position of 4 moves as the angle ψ changes, since 4 is also the center of the primary radius of curvature. L_3 is the variable distance between the secondary mirror and the second flat mirror. The beam is assumed to come vertically downward to the second flat from the first flat. The optical path at

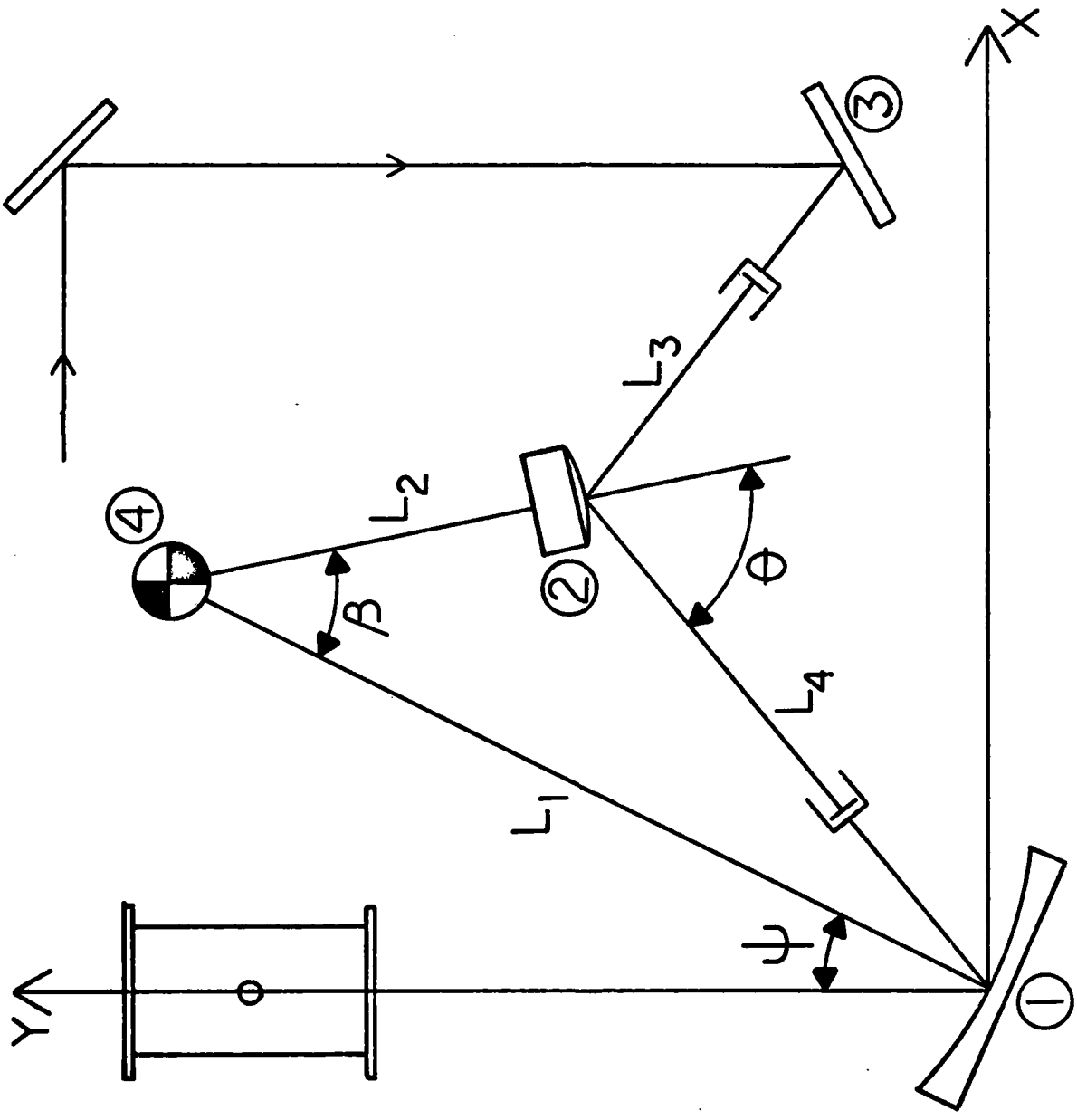

Figure 22 Mechanical Model of Optical System

all locations is assumed to be a line (so mirror curvature is not considered), and the angle of incidence is assumed to equal the exit angle.

Based on these assumptions, it should be clear that by specifying L_1, L_2, ψ, and X_3 (the X-location of the second flat), the position and orientation of the secondary mirror becomes fixed. Three implicit geometric relations are used:

$$\cos \beta = \frac{L_1^2 + L_3^2 - X_1^2 - Y_1^2}{2 L_1 L_3} \qquad (1)$$

$$\sin (90 + \psi - \beta) = \frac{L_3 \cos \psi - Y_1}{L_1} \qquad (2)$$

$$\sin (90 - 2\psi) = \frac{Y_1}{\sqrt{X_1^2 + Y_1^2}} \qquad (3)$$

In these relations, the three unknowns are β, X_2, and Y_2, where (X_2, Y_2) is the secondary mirror location. The three equations are solved simultaneously to solve for the secondary mirror position. From this, using β, the orientation Θ can also be found, as can the position and orientation of the flat mirrors. In practice, all that is necessary is to specify ψ and X_3 (whose maximum value is limited by interference from the test stand supports), then position the secondary mirror at its predicted location. This will produce a beam at the chamber having the desired F number and focal length. Of course, this model is only approximate, and some fine tuning of the optics will be necessary. But by knowing the approximate locations of the mirrors, the time and effort spent aligning the system should be kept to a minimum.

VII) References

1. Pirri, A. N., Monsler, M. J., and Nebolsine, P. E., "Propulsion by Absorption of Laser Radiation," AIAA Journal, Vol. 12, Sept. 1974, pp. 1254-1261.

2. Fowler, M. C., and Smith, D. C., "Ignition and Maintenance of Subsonic Plasma Waves in Air by CW CO2 Lawer Radiation...," Journal of Applied Physics, Vol. 46, Jan. 1975, pp. 138-150.

3. Henriksen, B. B., and Keefer, D. R., "Experimental Study of a Stationary Laser-Sustained Air Plasma," Journal of Applied Physics, Vol. 46, March 1975, pp. 1080-1083.

4. Fowler, M. C., "Measured Molecular Absorptivities for a Laser Thruster," AIAA Journal, Vol. 19, August 1981, pp. 1009-1014.

5. Kemp, N. H., "Simplified Models of CW Laser Heated Thrusters," AIAA Paper No. 81-1249, June 1981.

6. Conrad, R. W., Roy, E. L., Pyles, C. E., and Mangum, D. W., "Laser-Supported Combustion Wave Ignition in Hydrogen," Army Missile Command Technical Report Rh-80-1.

7. VanZandt, D. M., and McCay, T. D., "Experimental Study of Laser Sparks in Hydrogen," AIAA Paper No. 83-1443, June 1983.

8. Griem, H. R., Plasma Spectroscopy, McGraw-Hill, 1964

9. Abcock, B. D. and W. E. G. Plumtree, J. Quant. Spectros. Radiat. Trans., 4, 1964.

10. Lochte-Holtgreven, W., Plasma Diagnostics, North-Holland Publishing Co., 1968.

11. Key, J. F., J. W. Chan, and M. E. McIlwain, Welding Journal, Vol. 62, 1983.

12. Kobayashi, M. and T. Suga, Welding Institute Conference, Published by Welding Institute, U.K., 1982.

13. Tsao, K. C. and V. Pavelic, Welding Institute Conference, Published by Welding Institute, U.K., 1982.

14. Shumaker, J. B. and W. L. Wiese, Temperature, Vol. 3, C. M. Herzfeld (Editor), Reinhold, 1962.

15. Griem, H. R., Spectral Line Broadening, Academic Press, 1974.

16. Myronuk, D. J., and S. L. Soo, Int. Jour. Heat and Mass Trans., Vol. 14, 1981.

17. Keefer, D. R., B. B. Henriksen, and W. F. Braerman, J. of Appl. Physics, Vol. 46, No. 3, March 1975.

18. Barr, W. L., JOSA, Vol. 52, No. 8, Aug. 1962.

19. Thermophysical Properties of High Temperature Solid Materials, Vol. 4, Part 1, Purdue University 1967.

20. Kychakoff, G., R. D. Howe, and R. K. Hanson, Submitted to Applied Optics, August 1983.

21. Young, C. E., M. J. Pellin, D. M. Gruen, and J. H. Norem, J. Appl. Physics, 53 (7), July 1982.

22. Alden, M., H. Edner, Holmstedt, S. Svanberg, and T. Hogberg, Applied Optics, Vol 21, No. 7, April 1982.

23. Morley, C., Combustion and Flame, 47: 67-81, 1982.

24. Babelot, J. F., J. Magill, and R. W. Ohse, Temperature, Vol. 4, Part 1, American Institute of Physics 1982.

25. Cheng, T. K. and L. W. Casperson, J. of Appl. Physics Vol. 46, No. 5, May 1975.

END

FILMED

4-85

DTIC